https://doi.org/10.5194/egusphere-2026-2272
Preprint. Discussion started: 29 April 2026

Simulation of long-term peat accumulation dynamics & vulnerability: Insights from a Pole Forest and Palm Swamp in Amazonia

Yarin Tatiana Puerta[1], Ian T. Lawson[2], Steve Frolking[3], Greta Dargie[4], Jhon del Águila Pasquel[5], Christine Åkesson[2], Katy Roucoux[2], Eurídice N. Honorio Coronado[6], Gerardo Flores Llampazo[5], Timothy R. Baker[4], Mario A. Ruiz[8], and Adam Hastie[1,7]

[1]Department of Physical Geography and Geoecology, Charles University, Prague, CZ
[2]School of Geography and Sustainable Development, University of St Andrews, St Andrews, UK
[3]Department of Earth Sciences, University of New Hampshire, Durham, NH, USA
[4]School of Geography, University of Leeds, Leeds, UK
[5]Instituto de Investigaciones de la Amazonía Peruana, Iquitos, Peru
[6]Royal Botanic Gardens, Kew, Richmond, London, UK
[7]Department of Botany, Charles University, Prague, CZ
[8]Independent Researcher, Turin, Italy

Correspondence: Yarin Tatiana Puerta (puertaqy@natur.cuni.cz)

Abstract. Peruvian peatlands represent one of the largest reservoirs of carbon in Amazonia. This heterogeneous landscape exhibits several types of ecosystems, including pole forest (PF), palm swamp (PS), open peatlands (OP), and seasonal flooding forest (SFF). We apply the HPMTrop_EcoTy model, a novel development that represents ecological succession via bespoke parametrisations of ecohydrological mechanisms, to gain insights into long-term peat accumulation dynamics across these ecosystems and to assess their vulnerability to carbon gain and loss. Model results suggest that carbon accumulation rates in Amazonian peatlands are similar to or greater than those reported for the Congo Basin and Southeast Asia. Peat and carbon accumulation in Amazonia are particularly sensitive to local-scale changes, especially those driven by ecosystem succession. Amazonian peatlands appear less sensitive to precipitation changes, likely due to the extremely high rainfall across the Peruvian Amazon. However, reducing rainfall to levels similar to those of the present-day Congo Basin (45% reduction) produces an exponential decline in peat and carbon accumulation, suggesting a critical tipping point. Sensitivity analysis shows that PF, the most carbon-dense ecosystem, is the most sensitive, likely because it is rain-fed and therefore more vulnerable to ecohydrological changes, whereas SFF, the least carbon-dense, is the least sensitive. Considering the exceptionally high precipitation in the region, peatland formation appears mainly controlled by local processes such as river migration, which drives vegetation succession linked to peatland development.

1 Introduction

The Amazon basin hosts one of the largest peatland areas in the tropics, covering an estimated 251,000 km^2 (Hastie et al., 2024), compared with the Congo (160,000 km^2; Crezee et al., 2022) and Southeast Asia peatlands (248,000 km^2; Page and

https://doi.org/10.5194/egusphere-2026-2272
Preprint. Discussion started: 29 April 2026

Rieley, 2018). Peatlands are the result of a very slow process spanning thousands of years, during which vegetation material accumulates and decompose, a process regulated by climatic and hydrological conditions. Peat accumulation rates typically range from 1 to 13 mm year^{-1} (Page et al., 1999; Andriesse; Page et al., 2011; Lawson et al., 2026). The Amazon Basin has favourable conditions for peatland formation, including high annual precipitation (1,500 to 3,000 mm; Garcin et al., 2022; Lavado Casimiro et al., 2012), and extensive lowland topography prone to inundation. These factors, combined with autogenic succession and substantial river migration (up to $>$ 100 m year in western Amazonia; Quintana-Cobo et al., 2018; Kalliola et al., 1992), allowed for diverse peatland development throughout the Holocene, shaping their history and the wide variation in present-day vegetation (Kelly et al., 2020; Roucoux et al., 2013; Swindles et al., 2017).

Understanding how peat has accumulated over time can support hypotheses about the future of these ecosystems under land cover and climate change (Wang et al., 2018; Warren et al., 2016), and help guide effective conservation policies and strategies to mitigate carbon loss (Hastie et al., 2022). Important efforts have been made in this task for temperate peatlands (Frolking et al., 2010; Swinnen et al., 2019; Wang et al., 2016) as well as for tropical peatlands in Indonesia and the Congo (Kurnianto et al., 2014; Young et al., 2023). For Amazonia, one previous study did develop a model to represent peat accumulation in Peruvian peatlands (PMFB: Pastaza Marañón Foreland Basin); however this is a probabilistic model based on a statistical Bayesian and biogeochemistry approach (inferential) (Wang et al., 2018) rather than a mechanistic representation of peat accumulation (physical conceptual peat-core model) that includes ecological and hydrological process. Therefore, this work aims to address this research gap by adapting a dynamic peat model to be capable of representing the long-term processes of peat gain and loss in two different Peruvian peatlands.

In northwestern Amazonia, Peruvian peatlands cover an area of 62,714 km^2 (58,325-67,102 km^2) and store about 5.4 (2.6-10.6) Pg of carbon (Hastie et al., 2022). These peatlands may represent the most important peatland area in the Amazon Basin and some of the most carbon-dense ecosystems globally. They have been studied scientifically for over a decade, and some important data are available for understanding long-term peat formation across different ecosystem types. Two sites in particular have been studied in detail, Nueva York (NYO) and Veinte de Enero (VEN), which represent two different peatland ecosystems: a pole forest (PF) and a palm swamp (PS), respectively (Dargie et al., 2024). At each site, a peat core was collected from the centre of 0.5 ha forest plots. The core collected at NYO had a peat depth of 4.5 m and 6,175 years of age, while the VEN core reached 1.2 m of peat depth and 1,129 years of age (Åkesson et al. in prep.). Moreover, field studies have also been conducted at each site on net primary production, decomposition, and groundwater levels (Dargie et al., 2024), making them suitable for applying peat modelling while incorporating ecological data from the literature (del Aguila-Pasquel et al., 2013; Flores Llampazo et al., 2022; Honorio Coronado et al., 2021; Basuki et al., 2021; Hergoualc'h et al., 2023; Lähteenoja et al., 2009; Kelly; Lähteenoja et al., 2011).

This study applies and adapts HPMTrop, a one-dimensional peat-core model, to simulate peat accumulation (age-depth curve) in these two Peruvian sites. The model incorporates submodels for peat bulk density, decomposition, net primary productivity (NPP), water table (WT), and vegetation root addition, making it well-suited for Amazonian peatalnds that exhibit wide variability in all of these components. We adapt this model by representing the ecological succession of these Peru-

https://doi.org/10.5194/egusphere-2026-2272
Preprint. Discussion started: 29 April 2026

vian sites in terms of periods, using bespoke parameterisations. The overall objective is to gain insights into the patterns and sensitivity of peat and carbon accumulation. Specifically, the study has the following aims:

- Estimate long-term carbon accumulation rates which can be compared to other tropical regions, where similar modelling approaches have been applied.
- Identify the main drivers/controls on peat and carbon accumulation within these Amazonian peatlands.
- Evaluate tresholds, potential tipping points, and ecosystem sensitivity associated with changes in key drivers/controls of peat accumulation.

2 Materials and Methods

2.1 Sites

We configured HPMTrop for two peatland sites in northeastern Peru: Nueva York (4.401°S, 74.271°W) and Veinte de Enero (4.672°S, 73.819°W). Both sites are located within the Pastaza Marañón Foreland Basin (PMFB), an area of 120,00 km^2 known to be one of the most extensive peatlands in Amazon basin (Lähteenoja et al., 2011), with an estimated peat-carbon stock of 4.07 (1.94 -7.98) Pg C (Hastie et al., 2022). The basin hosts extensive floodplains and larger rivers such as the Marañón River, a whitewater river with hydrological order of 10 (Ríos-Villamizar et al., 2020), and one of the largest tributaries of the Amazon River (Figure1).

The site Nueva York (NYO-03) today a PF ecosystem is characterised by the dominance of pole thin-stemmed and large trees, as well as scattered palms. It is situated approximately **3.5 km from the Tigre river**, a blackwater left-bank tributary of the Marañón River. This site is a domed, ombrotrophic peatland, located far from active river margins, where precipitation is the main source of water input (Dargie et al., 2024; Draper et al., 2018). A permanent vegetation plot (NYO-03) was established at this site in 2014, and a 4.54 m peat core was collected in 2019. Radiocarbon dating of the basal peat yielded an age of 6,175 cal. yr BP. Pollen analysis, dry bulk density, and loss-on-ignition were also conducted on this core (*Åkesson et al., in prep*). The vegetation pattern in the initial stages of peat formation is characterised by palm vegetation (flooded Mauritiella-dominated palm swamp); in the middle to later stage by seasonally flooded forest mixed swamp forest, and palm swamp (Mauritiella- and Mauritia-dominated); and in the most recent stage by peatland pole forest (*Åkesson et al., in prep.*, see Figure S3). Similar vegetation changes have been described during the development of other present-day pole forests peatalnd in the PMFB (Kelly et al., 2020; Roucoux et al., 2013).

Veinte de Enero (VEN-02) is today a PS ecosystem, dominated by the palm *Mauritia flexuosa*. It is located approximately **1.4 km from the Yanayacu River**, a blackwater right-bank tributary of the Marañón River, and about **3 km from the Marañón** itself (Dargie et al., 2024). VEN-02 receives water and nutrient inputs from river flooding. The water table levels fluctuate much more at VEN-02 than at NYO-03 (Flores Llampazo et al., 2022). VEN-02 has a concave topography, indicating a less developed peatland structure than the NYO-03 ecosystem. A 1.23 m peat core was obtained, with radiocarbon dating indicating

https://doi.org/10.5194/egusphere-2026-2272
Preprint. Discussion started: 29 April 2026

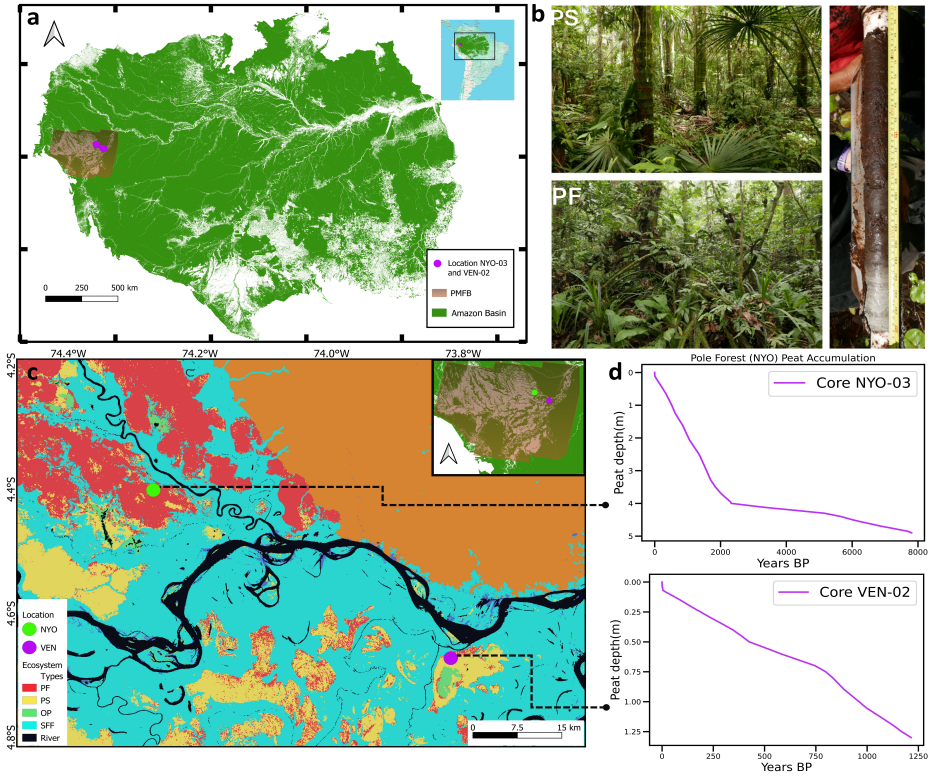

Figure 1. Location of Nueva York (NYO-03; Pole Forest = PF) and Veinte de Enero (VEN-02; Palm Swamp = PS) in Peruvian Forest, northwestern Amazon Basin. (a) The Amazon Basin with the Pastaza Marañón Foreland Basin (PMFB), source: Hastie et al. (2024)). (b) Images of a Pole Forest (PF), a Palm Swamp (PS), and a peat core sample showing the transition between peat and grey clay at 2.6m, source: this an example from another Peruvian peatland by Lawson et al. (2022). (c) Locations of the NYO-03 (PF) and VEN-02 (PS) forest plots within the Pastaza Maranon Foreland Basin (PMFB) and the distribution of different ecosystem types: pole forest (PF), palm swamp (PS), seasonal flooded forest (SFF), and open peatland (OP), source: Hastie et al. (2022). (d) Age-depth curve based on radiocarbon age determinations on bulk peat from NYO-03 and VEN-02 peat cores, using the Rbacon package version 2.5.7 and the IntCal20 calibration curve, source: *Åkesson et al., in prep.*

.

a basal peat age of 1,129 cal. yr BP. Pollen analysis, dry bulk density, and loss-on-ignition were also conducted on this core. The vegetation succession is characterised by open vegetation in the initial stages and culminates in the present-day peatland palm swamp dominated by *Mauritia* (*Åkesson et al., in prep.*; see Figure S4 in Supplementary Information).

2.2 Model application description:

The HPMTrop (Kurnianto et al., 2014) is a modified version of the original HPM (Frolking et al., 2010) to simulate peat accumulation in tropical ecosystems (Appendix A Figure A8). It is a one-dimensional model that operates on a monthly time

https://doi.org/10.5194/egusphere-2026-2272
Preprint. Discussion started: 29 April 2026

step, using precipitation as the driving data to simulate water table (WT) fluctuations. The model processes newly accumulated peat into annual cohorts (spatial reference of one year of peat accumulation represented as a vertical slice of peat column), which is estimated by the balance between litter input and the decomposition rate regulated by WT fluctuation.

To run the model for each site described above, we incorporated a simulation approach by successional periods (see section 2.2.1). This required an understanding of the ecological history of each site based on vegetation succession reconstructed from pollen data (*Åkesson et al., in prep.*). The result is a classification of the dominant Ecosystem Type (EcoTy) across different time periods throughout the simulation. Each site transitioned through different EcoTy (e.g., PS -> PF), therefore, the HPMTrop parameterisations were adjusted to support simulations across multiple periods and EcoTy to reflect the conditions during each time period (see Appendix A Figure A1-A2). The result of this adaptation is the HPMTrop_EcoTy model, which is a novel development that represents ecological succession via bespoke parametrisations of ecohydrological mechanisms.

The litter input is determined by the relationship between plant productivity (NPP) and WT position (See section 2.2.3), based on an empirical relationship obtained by EcoTy (i.e. NPP and WT data from each type of ecosystem). This input is discriminated for plant functional types (PFTs) such as palms, trees and grasses. And each PFT is divided into above-ground (leaves, stem, and wood) and below-ground (fine and coarse roots) biomass components (Dargie et al., 2024). The decomposition of both accumulated peat and newly added litter depends on the position of WT. Decomposition occurs more slowly below the WT and more rapidly above it, as regulated by the interaction between peat accumulation and the WT fluctuation (See Eqs. 5 and 7 to 9 in Frolking et al., 2010).

Net peat accumulation and its rate over time are governed by the balance between litter input and decomposition, both of which are strongly influenced by WT variability (Clymo; Frolking et al., 2001, 2010). Site-specific sub-models to represent water table dynamics for each EcoTy was developed (see section 2.2.2).

A central assumption of the modelling approach developed in this study is that the current parameter values of different EcoTy can be used to represent past conditions for the same EcoTy. This assumption is supported by chronosequence and palaeoecological research, which suggests that vertical (temporal) vegetation gradients observed in peat cores are analogous to present-day horizontal vegetation gradients (e.g. with distance from river). In other words, past vegetation assemblages likely responded to environmental conditions similarly to those observed today (Kelly et al., 2017; Roucoux et al., 2013; Tuittila et al., 2012).

All parameter values used in the HPMTrop_EcoTy and a complete description of each parameter about how it was obtained, sources and calculations, are detailed in the Table HPMTrop_EcoTy_Parameters.xlsx (See codedataavailability). For the model calibration process, we used the peat core samples from NYO-03 and VEN-02, along with their corresponding age-depth curves (reference curves) derived from palaeoecological reconstruction models using the rbacon package in R and calibrated basal radiocarbon dates (*Åkesson et al., in prep.*). The reference curves were used to compare the simulated age-depth curves (model output) and to adjust the model parameters until a good fit was achieved between the simulated and reference curves.

https://doi.org/10.5194/egusphere-2026-2272
Preprint. Discussion started: 29 April 2026

Table 1. Definition of range of periods and the corresponding EcoTy by site

Site	Periods	Age (cal. yr BP)	EcoTy	Duration (yr)	Lab Code
NY0-03	1	4917-6175	PS	1259	NYO-03_2018_IntCal20
	Transition 1 to 2	4147-4917	PS to SFF	770	
	2	1646-4147	SFF	2501	
	Transition 2 to 3	1436-1646	SFF to PS	210	
	3	216-1436	PS	1220	
	Transition 3 to 4	166-216	PS to PF	50	
	4	0-166	PF	166	
VEN-02	1	946-1129	OP	183	VEN-02_2018_IntCal20
	Transition 1 to 2	589-946	OP to PS	357	
	2	0-589	PS	589	

Note: Lab code is provided for age-depth curve reconstruction (Åkesson et al., in prep.). Age calendar years before present (cal. yr BP). Pole Forest (PF), Palm Swamp (PS), Open Peatland (OP), Seasonal Flooded Forest (SFF).

2.2.1 Ecosystem type dynamics

For each site we have pollen data to trace the history of vegetation changes (*Åkesson et al., in prep.*). We used the presence of conspicuous vegetation to identify distinct ecological stages (See Appendix A Figure A3-A4). These stages were defined as **simulation periods** (see Table 1).

Each period corresponds to a distinct EcoTy, characterised by one or more representative plant taxa (e.g., a phase of *Mauritia* dominance) (*Åkesson et al., in prep.*, Kelly et al., 2017, 2020). The transition from one EcoTy to another was identified by shifts in relative abundance of the species in the pollen diagram, where decreases in representation of one group of plants (e.g., palms) and increases in another (e.g., grasses) indicated an ecological change. The interval during which these changes occur was defined as a transition period. During this time, the parameters representing the initial ecosystem gradually shift towards those representing the subsequent ecosystem, reflecting a gradual (linear) rather than abrupt change into the model. From the pollen data we cannot infer how this transition occurs in terms of mechanism, therefore we assumed a linear transition over the defined transition period.

The results obtained from the simulation are presented according to the four EcoTy considered into the model: pole forest (PF), palm swamp (PS), open peatlands (OP), and seasonal flooding forest (SFF). The NYO-03 site-currently a PF and the oldest of the two, was represented by three ecosystem types: PS, SFF, and PF across four periods (and three transition periods), with PS occurring in two distinct periods. The VEN-02 site-currently a PS, was represented by two ecosystem types: OP and PS, over two periods (and one transition period). Figure A1-A2 (Appendix A) illustrate the simulation evolution for each site.

https://doi.org/10.5194/egusphere-2026-2272
Preprint. Discussion started: 29 April 2026

2.2.2 Precipitation and Water Table reconstruction

Holocene precipitation data used as the climatic forcing variable in the model were obtained from the CCSM3 (TraCE-21ka) simulation at a spatial resolution of 3.75° x 3.75°. Monthly precipitation values were derived from the CCSM3 time series bias-corrected using observed precipitation from ground data from meteorological stations recorded by SENAMHI (Servicio Nacional de Meteorología e Hidrología del Perú). A fixed multiplicative correction factor was applied for each calendar month to adjust the simulated precipitation amounts (more details Appendix A Text A1).

To simulate WT fluctuations, we developed an empirical statistical model (eq.2) based on site-specific data such as precipitation (P) in mm from two meteorological stations (Bagazan-VEN-02 and Santa Rita-NYO-03) and flux tower data (PE-QFR) (Griffis et al., 2020), and in situ WT measurements using data loggers recording between 2018 and 2020 (Dargie et al., 2024; Flores Llampazo et al., 2022). WT levels were correlated with the cumulative monthly water deficit (WD) (See Table HPMTrop_EcoTy_Parameters.xlsx and Appendix A Figure A7), following a common equation (eq. 1) for tropical forest ecosystems (Malhi et al., 2009; Hutyra et al., 2005; Frolking et al., 2011; Aragão et al., 2007), and using the same approach described by Kurnianto et al. (2014).

$$WD_i(mm) = \max(0, WD_(i-1) + [E(mm) - P(mm)]) \quad (1)$$

Where, $WD =$ cumulative monthly water deficit in mm, $E =$ evapotranspiration, for Amazon is assumed 100 mm month-1 (Aragão et al., 2007; Griffis et al., 2020), $P =$ precipitation in mm from CCSM3(TraCE-21ka) corrected, and i = month.

$$WT(cm) = a \times WD(mm) + b \quad (2)$$

2.2.3 Net Primary Production

Net primary productivity (NPP) values for the PS and PF ecosystem types, were derived from field data from both sites: VEN-02 (PS) and NYO-03 (PF) by Dargie et al. (2024). For the SFF and OP ecosystem types, NPP values were obtained from the literature (del Aguila-Pasquel et al., 2013; Basuki et al., 2021). For PF and PS, we have NPP values for tree components, i.e. leaves, stem, roots, and for palms components (leaves and roots). For SFF we only find NPP values for tree components (leaves, stem, roots), and for OP we considered only grasses components (leaves and roots). All of these values, derived from field data and literature, are used as initial NPP values in the model (Appendix A Table A1).

Into the model, NPP is recalculated every month using a submodel, which is a function of the WT. Several studies have shown that NPP is correlated with WT levels through a quadratic relationship (Hirano et al., 2012; Sousa et al., 2022). Both excessive flooding and prolonged water deficits negatively affect vegetation growth and productivity. We developed an empirical model between NPP and WT for each EcoTy. A quadratic regression was fitted and integrated into HPMTrop_EcoTy to estimate NPP as a function of WT (See Table HPMTrop_EcoTy_Parameters.xlsx).

https://doi.org/10.5194/egusphere-2026-2272
Preprint. Discussion started: 29 April 2026

In the model NPP is divided into two fractions: above ground (AB) and below ground (BG). AB is the NPP input from leaves and stem, which is added to the peat profile at the surface. BG is the input from roots, which is added uniformly to the peat profile up to a predetermined depth value (rootin_depth from Table HPMTrop_EcoTy_Parameters.xlsx).

2.2.4 Decomposition and peat properties

The initial decomposition values in the model come from in-situ litter bag experiments from both sites (VEN-02 (PS) and NYO-03 (PF) by Dargie et al., 2024). For the other EcoTy (SFF and OP), exponential decay values were obtained from literature for each PFT and component (Appendix A Table A2). Parameters related to bulk density were derived from various studies (Appendix A Figure A5) (Honorio Coronado et al., 2021; Lähteenoja et al., 2011, 2009; Kelly). Other density parameters (dens_c1 and dens_c2, from Table HPMTrop_EcoTy_Parameters.xlsx), were initially estimated using curve-fitting techniques and then fine-tuned through calibration. An empirical model for decomposition rate and data from literature was used to derive the soil properties values represented in the model with the Water Filled Pore Space (WFPS) (see Appendix A Figure A6, and Frolking et al., 2010).

2.2.5 Sensitivity analysis

A sensitivity analysis was performed by varying key parameters $\pm 25\%$ and tracking the response of the key variables peat depth and carbon content. We run HPMTrop with changes in precipitation (P), NPP, and initial decomposition rate (k). After this first analysis, a sensitivity analysis was conducted by progressively changing precipitation in 5% steps, from 25% up to 45%, to identify potential tipping points in peat accumulation by EcoTy at the two simulated sites. Up to 45% reduction in precipitation is considered a plausible outcome under conditions of deforestation and savannisation according to projections (Bottino et al., 2024; dos Reis et al., 2021).

3 RESULTS

3.1 Peat age-depth curve, carbon and peat accumulation rates

The simulated peat depth curve reached 4.56 m over 6,175 years at the NYO-03 site and 1.18 m over 1,129 years at the VEN-02 site. These results were compared with the reference age-depth curves and the final peat depths recorded in the cores, which were 4.54 m (6,175 cal. yr BP; Figure2) for NYO-03 and 1.23 m (1,129 cal. yr BP; Figure2) for VEN-02. Although the simulated final depths closely match the core values, there are differences between the slopes of the simulated and reference age-depth curves. For NYO-03 the main slope differences occur between 2,000 and 800 cal. yr BP, when the reference curve is slightly steeper than the simulated (EcoTy simulated: PS); and between 6,175 and 5,000 cal. yr BP when the reconstructed curve again shows a slightly greater slope than the simulated curve (EcoTy simulated: PS). For VEN-02, notable differences appear between 400 and 0 cal. yr BP, where the simulation produces a concave curve in contrast to the straight reference curve

https://doi.org/10.5194/egusphere-2026-2272
Preprint. Discussion started: 29 April 2026

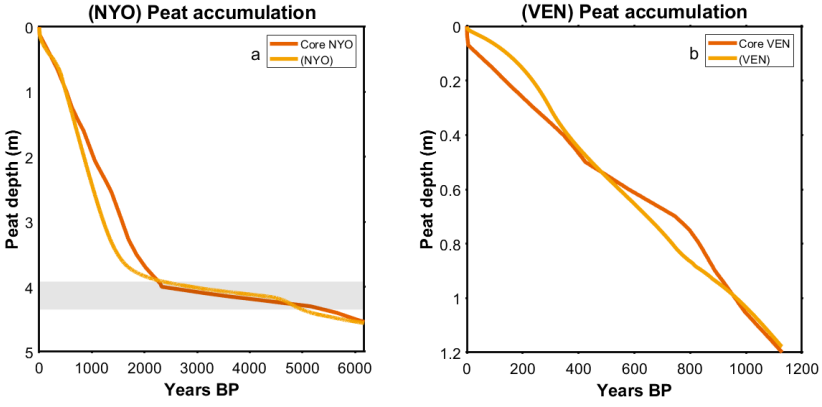

Figure 2. Peat depth by site. Simulated and reference age-depth curves for NYO-03 (a) and VEN-02 (b) sites. The yellow line represents the simulated age-depth curve from HPMTrop_EcoTy, while the orange line indicates the reference age-depth curve derived from palaeoecological reconstruction approach. The shaded area in (a) plot denotes the hiatus period or slow peat accumulation in NYO-03. The y-axis shows peat depth in meters and the x-axis represents age in years before present (Years BP).

(EcoTy simulated: PS), and between 950 and 600 cal. yr BP, where a similar pattern is observed (EcoTy simulated: Transition from OP to PS).

With respect to accumulation rates derived directly from the peat height profiles for each site (Figure3), the mean peat and carbon accumulation rates were 0.70 mm y^{-1} and 29.13 g C m^{-2} y^{-1}, respectively, at NYO-03, and 1.04 mm y^{-1} and 49.89 g C m^{-2} y^{-1} of carbon, respectively at VEN-02. Table 2 presents the specific peat and carbon accumulation rate by EcoTy, along with the duration of dominance for each ecosystem in both simulations. Notably, results for SFF indicate substantial reduction in peat accumulation, with a rate of 0.06 mm y^{-1} and carbon accumulation rate of 3.76 g C m^{-2} y^{-1}.

For NYO-03, the simulated peat height (Figure3) increased by 1.0 m during the first 1,259 years (4,917-6,175 cal. yr BP). Over the following 800 years (4,147-4,917 cal. yr BP), peat height decreased to 0.8 m. Between 4,147 and 1,436 cal. yr BP (2,700 years), peat accumulation was minimal with a peat height increasing only slightly to 1.0 m. During the last 1,400 cal. yr BP up to the present, peat height increased by around 3.5 m, reaching a total thickness of about 4.6 m. This most recent interval presents the highest rates of peat accumulation in the NYO-03 site simulation.

For VEN-02 site, the simulated peat height (Figure3) increased rapidly by 0.8 m during the first 500 years (589-1129 cal. yr BP). In the final 589 years of the simulation (0-589 cal. yr BP) peat height increased by 0.3 m, reaching a total thickness of 1.2 m.

https://doi.org/10.5194/egusphere-2026-2272
Preprint. Discussion started: 29 April 2026

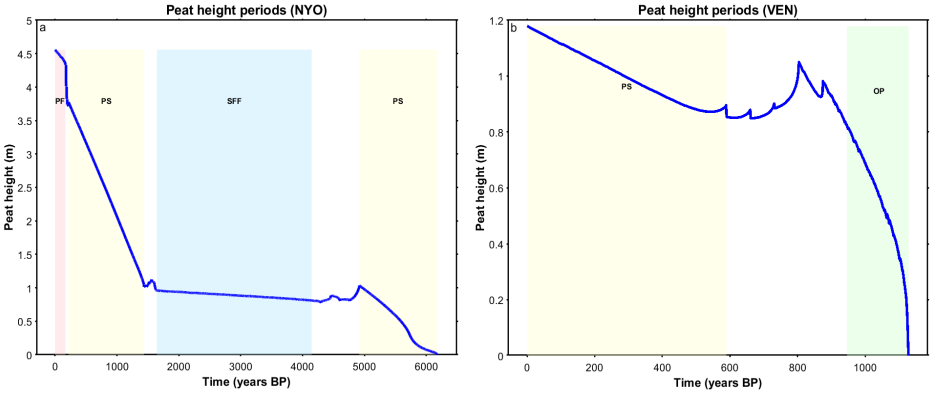

Figure 3. Peat height by site. Peat height for NYO-03 (a) and peat height for VEN-02 (b). The colour shadow areas represent the different EcoTy that were simulated across each site. The light-red corresponds to Pole Forest (PF), the light yellow corresponds to Palm Swamp (PS), the blue corresponds to Seasonal Flooded Forest (SFF), and the light-green corresponds to Open Peatland (OP). The white spaces between colours correspond to transition periods between two EcoTy. The y-axis shows peat height in meters, and the x-axis represents time in years before present (Years BP).

3.2 Periods by ecosystem types:

At NYO-03 site the average NPP and decomposition fluxes (all in kg C m^{-2} y^{-1}) during the first millennium indicated a net positive period, with NPP 0.70 and the decomposition rate 0.56. During the subsequent millennia, NPP increased to 0.86 as well as the decomposition rate, however, this resulted in net negative balance (likely due to secondary decomposition and the effect of the transition period, i.e., linear change in parameter values). Over the following two millennia, NPP and decomposition rate were both 0.89, this time, resulting in a positive balance with slight net gain (likely due the transition of a stable period, i.e., stable parameter values). During the subsequent two centuries, NPP declined to 0.78 and decomposition rate 0.80, leading a net negative balance. In the last millennia NPP and decomposition presented a positive balance, with values 0.68 and 0.59 respectively (Table 2). Variations in both fluxes was driven mainly by the WT dynamics (see Appendix A Figure B1).

At VEN-02 site the average NPP and decomposition fluxes (kg C m^{-2} y^{-1}) over the entire simulation resulted in a net positive balance, with an NPP of approximately 0.80 and decomposition rate 0.75 (Table 2). The OP period exhibited higher productivity (NPP of 1.01) than the PS period (NPP of 0.70).

Productivity rate at both sites varied depending on the ecosystem type and plant functional component. Across the entire simulation total NPP was 7.0 Mg C ha^{-1} y^{-1} for NYO-03 and 8.0 Mg C ha^{-1} y^{-1} for VEN-02 (2). At the end of the simulation the total peat carbon stocks was 1,799.4 Mg C ha^{-1} at NYO-03, accumulated over 6,175 years, and 563.1 Mg C ha^{-1} at VEN-02, accumulated over 1,129 years. The productivity by EcoTy (Total NPP Mg C ha^{-1}) indicated that OP was

https://doi.org/10.5194/egusphere-2026-2272
Preprint. Discussion started: 29 April 2026

the most productive ecosystem, followed by SFF and PS, and finally PF as the least productive. In terms of component, leaves represent the main input to NPP, followed by roots, particularly palms and grass fine roots (Appendix B Table B1).

3.3 Sensitivity analysis

In general, the NYO-03 site exhibited more sensitivity than the VEN-02 site (Appendix B Figure B3). The parameters which most influenced final peat depth and carbon accumulation were NPP and initial decomposition rate (K) (see Figure 4).

When NPP was increased by 25%, final peat depth rose by 79% at NYO-03 and 48% at VEN-02. Conversely, a 25% decrease in NPP reduced final peat depth by 49% at NYO-03 and 30% at VEN-02. When K was increased by 25%, final peat depth decreased by 30% at both sites. However, when K was reduced by 25%, final peat depth increased by 77% at NYO-03 and 71% at VEN-02.

In terms of P, a $\pm$25% change did not produce major alterations in final peat depth or carbon accumulation compared with the other parameters at either site. Nevertheless, the NYO-03 site showed a more noticeable response, particularly under decreased precipitation. However, further decreases in P (beyond 30%) produced a dramatic response.

At NYO-03, increasing precipitation by 30%, 35%, 40%, or 45% practically produced no alterations in final peat depth or height. For example, when precipitation was increased 45% result in a very slight increase in peat depth from 4.56 to 4.61 m. In contrast, decreasing precipitation beyond 30% led to reductions in final peat depth with an exponential decline. The maximum precipitation reduction of 45% resulted in 52% decrease in peat depth. For the VEN-02 site, a similar pattern was observed in response to changes in precipitation. The maximum alteration was a 32% decrease in peat depth under a 45% in precipitation reduction. This analysis highlights a clear distinction in sensitivity to precipitation changes, particularly decreases, with the NYO-03 site being more sensitive to reduced precipitation than VEN-02 site (Appendix B Figure B6). A more detailed description by parameter and EcoTy are provided in the Appendix B Text B1.

4 DISCUSSION

4.1 NPP and WT

Several studies have evidenced a quadratic relationship (hump-shaped) between WT and NPP. In general, productivity decreases when the WT is either too shallow or too deep (Hirano et al., 2012; Mezbahuddin et al., 2014; Sousa et al., 2022). Thus, high productivity is typically achieved under intermediate WT conditions. In our model a quadratic relationship was incorporated into the monthly NPP calculations by EcoTy. However, the PF ecosystem exhibited a delayed response to changes in monthly WT variability, with an estimated lag of approximately three months. Souza et al. (2022) report the same lag for other forests on Amazon. In contrast, PS, OP, and SFF respond more rapidly. The delayed response in the PF vegetation could be associated with the stability of the ecosystem. PF may buffer WT fluctuations, with its hummock topography, delaying impacts on productivity. The lag between NPP and WT in PF appears plausible with its ecological characteristics; however,

https://doi.org/10.5194/egusphere-2026-2272
Preprint. Discussion started: 29 April 2026

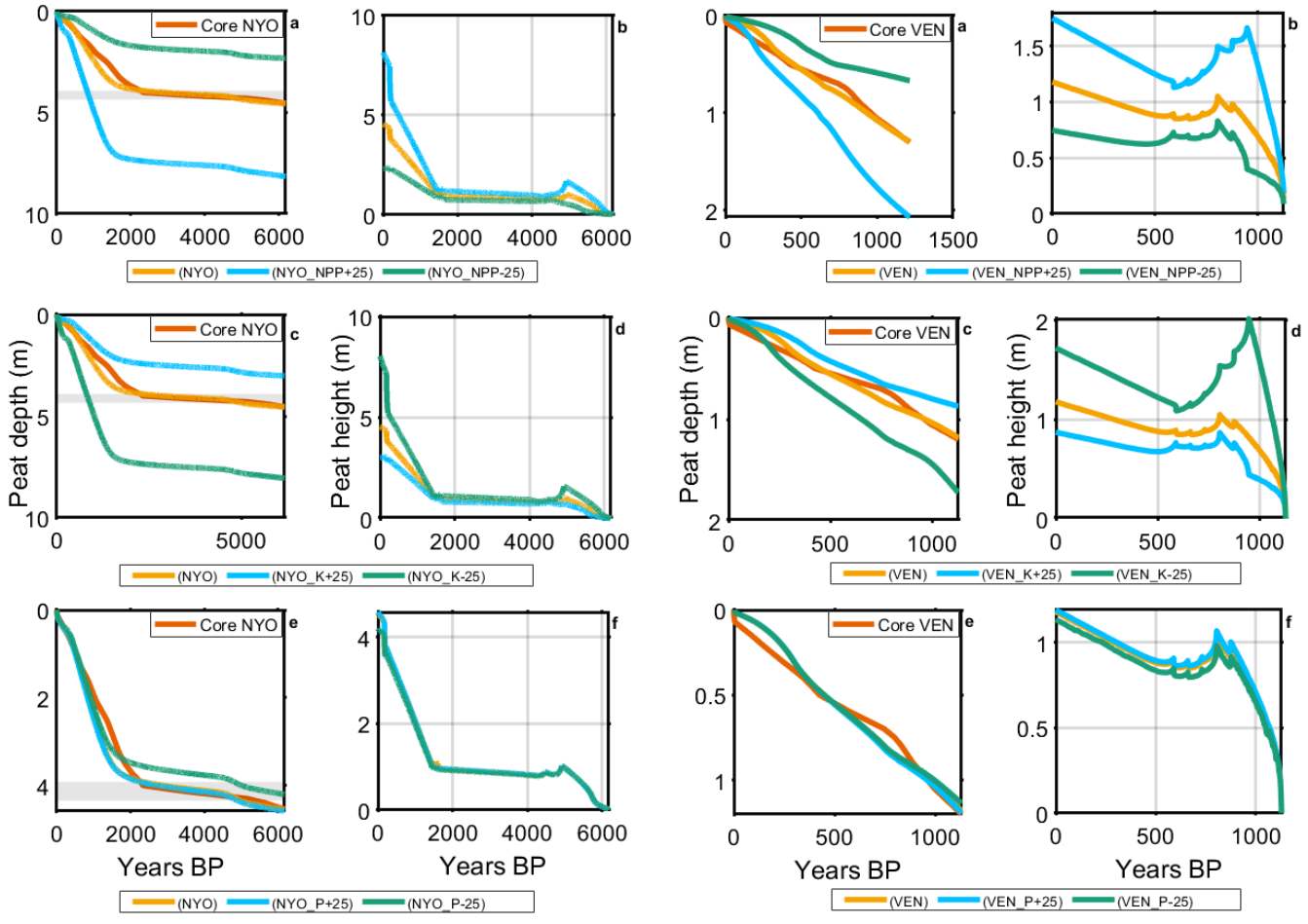

Figure 4. Model sensitivity analysis for NYO-03 (left side) and VEN-02 (right side). The simulated age-depth curve is compared with the core reference curve (line in orange colour). The gray rectangular shaded patch indicates the hiatus during the middle Holocene. The yellow line is the simulation base. The blue line is the +25% change and the green line is the -25% change for each parameter. The a, c, e plots corresponds to peat depth and the b, d, f plots to peat height. The sensitivity to changes in Net primary productivity (NPP) is shown in plots a and b, for decomposition (K) is shown in the plots c and d, and for precipitation is shown in plots e and f.

https://doi.org/10.5194/egusphere-2026-2272
Preprint. Discussion started: 29 April 2026

due to the limited time series available, this conclusion remains speculative and should be validated with additional data or a more robust NPP-WT model (physical instead of statistical).

All ecosystems present in the Peruvian Amazon exhibit high productivity rates (Draper et al., 2018; Honorio Coronado et al., 2021). In the simulation, OP and SFF showed the highest productivity, followed by PS and PF. In our simulation OP was assuming grasses which can support faster productivity than trees or palms (As Morison et al. (2000) showed grasses present higher photosynthetic efficiency). The results highlighted that roots, especially those associated with palms and grasses (fine roots) contributed to high NPP in PS and OP respectively. The lowest productivity in the simulation was the PF ecosystem, which is consistent with prevailing understanding of PF being the most stable ecosystem in terms of WT fluctuation (Flores Llampazo et al., 2022), having more acidic and nutrient-poor conditions, and being dominated by thin-stemmed wood (Honorio Coronado et al., 2021).

The simulation estimated a relatively similar mean productivity of 6.7 and 8.0 Mg C ha^{-1} y^{-1} for NYO-03 and VEN-02 respectively. The difference could be associated not only with the litter inputs but also with site age, successional history, and water table dynamics. Average NPP by EcoTy showed that PF (5.8 Mg C ha^{-1} y^{-1}) exhibited lower NPP than PS (7.0 Mg C ha^{-1} y^{-1}), congruent with (Dargie et al., 2024)'s study that reveals the same pattern (7.34 $\pm$ 0.84 Mg C ha^{-1} y^{-1} for PF; 9.83 $\pm$ 1.43 Mg C ha^{-1} y^{-1} for PS). This supports the fact that even with a simple NPP model the overall productivity trend in both ecosystems is being captured.

Higher NPP in PS may be linked to the contribution of fine roots. Previous studies have shown that soil organic carbon increases with diversity of fine roots (Chen et al., 2023) and Dargie et al. (2024) also highlighted the important contribution of this component into total NPP. Although the model does not incorporate chemical traits of the different compounds, the even root addition and the higher initial NPP values, could be key factors driving the higher productivity simulated for PS relative to the other ecosystems.

4.2 WT, peat and carbon accumulation rates

Even with a simplified representation of the WT, the simulation maintains a conservative range of fluctuation representative of each EcoTy, similar to the pattern of WT fluctuation reported by Flores Llampazo et al. (2022) in the same EcoTy. WT fluctuations and river migration are crucial factors of ecosystems dynamic in the Amazon. As Swindles et al. (2017) suggested long-term shifts among EcoTy are a common process that results in both gains and losses of net peat, particularly during drought events or transitions between ecosystems. In our simulation of the **NYO-03 site**, peat and carbon losses, reflected in negative accumulation rates, occurred during transition periods, but, the fastest peat gains occur also in transitions. Our simulation suggests that the rate of peat accumulation depends on the specific ecosystem transition and stable period.

At NYO-03 the loss transition period occurred from PS to SFF (4,147 to 4,917 cal. yr BP), with peat and carbon rates of -0.28 mm y^{-1} and -4.71 g C m^{-2} y^{-1} respectively; resulting in a reduction of 0.2 m in peat height. The loss could be associated with changes in WT variability. This transition implies a drop in mean WT, leading the model to simulate aerobic conditions and thereby accelerating the decomposition. As long-term decomposition experiments highlight the importance of waterlogged conditions for peat formation and carbon stocks (Perryman et al., 2026). This result is consistent with the onset of

https://doi.org/10.5194/egusphere-2026-2272
Preprint. Discussion started: 29 April 2026

a hiatus in the reference curve from the core, and with negative peat accumulation rates reported by Swindles et al. (2017) for another peatland in Peruvian Amazon during approximately the same time.

Under the SFF ecosystem (1,646-4,174 cal. yr BP), the simulation suggests a hiatus in peat accumulation, consistent with prevailing understanding that SFF are rarely peat-forming (Honorio Coronado et al., 2021; Flores Llampazo et al., 2022). Nevertheless, the peat accumulation rate is not zero, but on average remains very low (0.06 mm y^{-1}). This pattern is associated with the shift from a typical peat-forming conditions (PS) to a rare or non-peatland forming system (SFF), that in the model is driven mainly by the deeper WT in the SFF ecosystem. As Garcin et al. (2022) suggests, once conditions stabilise again (in this case, after the transition from PS to SFF), peat accumulation can resume; however, the conditions within SFF are not sufficiently favourable to sustain high peat accumulation rates. Remarkably, this period coincides closely with the *"ghost interval"* reported by Garcin et al. (2022) and Young et al. (2021), in which massive peat loss in the Congo was primarily attributed to a dry period between 5,000 and 2,000 cal. yr BP. While, the absence of peat accumulation in our case (our "ghost interval") could also be linked to drier conditions, the results of our sensitivity analysis, combined with the predominance of high precipitation in the Amazon (3,000 mm y^{-1}) and the strong influence of river migration in the Eastern Amazon, provide evidence to cast doubt on the drought-only hypothesis. Although we do not completely dismiss the drought hypothesis, our model results, together with the ecological history of the Amazon, point to local factors as key drivers of natural peat loss and accumulation processes. Another important point is that, unlike the Congo ghost interval where peatlands became a source of carbon, in our simulation the SFF remained a carbon sink. This is likely due to the consistently high precipitation in the Amazon, which maintains a relatively high WT even during the SFF period, preventing extensive peat decomposition.

In the next transition period the peat accumulation rate increases to 0.3 mm y^{-1} (1,436-1,646 cal yr BP), however, the carbon accumulation rate becomes negative (-15.5 g C m^{-2} y^{-1}). This suggests that even with a positive peat accumulation, the transition period (non-stable conditions) leads to carbon loss likely resulting from a negative Net Carbon Balance (NCB; see Figure 5) (Frolking et al., 2014). As demonstrated by Young et al. (2021), even when peat is gained, the decomposition of older peat can continue, producing a delayed effect that drives a negative carbon balance. In our simulation after nearly 3,000 years under SFF conditions (deeper WT), the transition from this ecosystem to PS resulted in a loss of carbon. Even under wetting conditions, the addition of new peat (positive peat accumulation rate) could lead to an overall lower bulk density due to the input of fresh peat, however cannot offset the carbon loss (negative carbon accumulation rate). At the subsequent stable PS period (216-1,436 cal. yr BP), both peat and carbon accumulation rates become positive again (2.3 mm y^{-1} and 96.2 g C m^{-2} y^{-1} respectively), indicating a recovery of the ecosystem.

In this simulation the highest accumulation rates were observed during transitions from PS to PF (166-216 cal. yr BP; 11.3 mm y^{-1}). This occurred likely due to less peat being decomposed (more superficial WT position) allowing the newly deposited material to accumulate more rapidly, and temporarily boosting the peat accumulation rate until the new stable period is reached (as Kurnianto et al. (2014) described lack of time and conditions for decomposition could increase peat accumulation rate). The final period of the NYO-03 simulation from the present to 166 cal. yr BP, represents the current PF EcoTy with a peat accumulation rate of 1.3 mm y^{-1}.

https://doi.org/10.5194/egusphere-2026-2272
Preprint. Discussion started: 29 April 2026

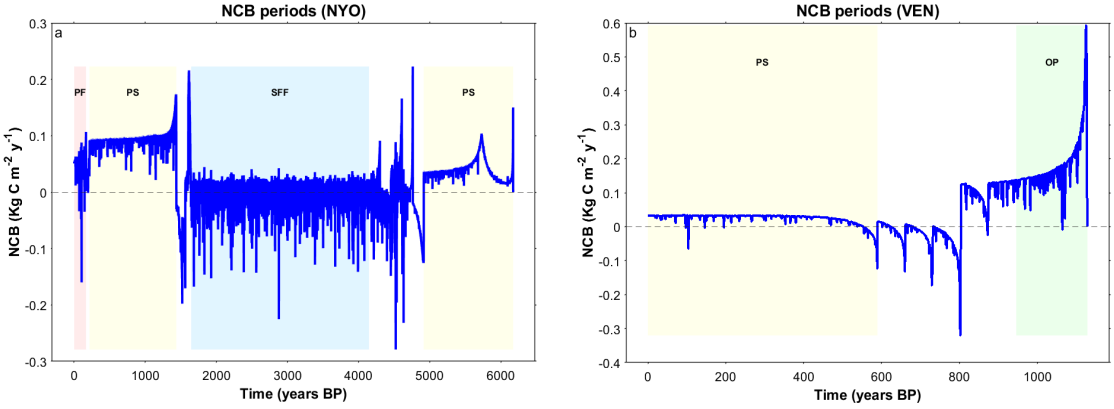

Figure 5. Net carbon balance (NCB). Simulated net carbon accumulation rate for NYO-03 (a) and for VEN-02 (b). The colour shadow areas represent the different EcoTy that were simulated across each site. The light-red corresponds to Pole Forest (PF), the light yellow corresponds to Palm Swamp (PS), the blue corresponds to Seasonal Flooded Forest (SFF), and the light-green corresponds to Open Peatland (OP). The white space between colours correspond to transition periods between two EcoTy

For **VEN-02** simulation, the single transition period from OP to PS (589-946 cal. yr BP) resulted in average in a positive peat and carbon accumulation rate (0.1 mm y^{-1} and 27.2 g C m^{-2} y^{-1}, respectively). This is likely because the OP ecosystem has the highest peat accumulation rate and WT remains the same during the entire simulation. Thus, the transition to PS still maintains favourable conditions for peat accumulation. The stable subsequent period PS (0-589 cal. yr BP) exhibited positive peat and carbon accumulation rates (0.5 mm y^{-1} and 24.3 g C m^{-2} y^{-1}).

All peat and carbon accumulation rates obtained in both simulations during stable periods (excluding SFF and transition periods) ranged from 0.5 to 4.5 mm y^{-1} and 24.33 to 177 g C m^{-2} y^{-1} respectively, and are comparable with ranges reported for the PMFB. Lawson et al. (2026) reported 0.21 to 2.58 mm y^{-1}, while Lähteenoja et al. (2009) reported a historical yearly rate of peat accumulation of 0.94 $\pm$ 0.99 to 4.88 $\pm$ 1.65 mm and 26-195 g C m^{-2}. Wang et al. (2018) reported average SOC accumulation rates of 55.98 g C m^{-2} y^{-1} (range 29-85) with higher rates in PS and OP (64 and 29 g C m^{-2} y^{-1}, respectively). Controversially, Lähteenoja et al. (2009) reported a PF (San Jorge) as having one of the highest average carbon accumulation rate (85 g C m^{-2} y^{-1}) compared with OP and PS. And Swindles et al. (2017) reported a high carbon accumulation rate in another PF (Aucayacu; 71 g C m^{-2} y^{-1}).

In our simulation, consistent with Lähteenoja et al. (2009) and Swindles et al. (2017), the PF ecosystem exhibited relatively high carbon accumulation rates along with OP, at 56.8 and 177.2 g C m^{-2} y^{-1}, respectively, although OP is the ecosystem with the greatest uncertainty in the simulation. This was followed by PS with 53.2 g C m^{-2} y^{-1} (range 24-96) (Appendix B

https://doi.org/10.5194/egusphere-2026-2272
Preprint. Discussion started: 29 April 2026

Figure B2). Overall, the average carbon accumulation rate across all EcoTy was 72.7 g C m^{-2} y^{-1}, remaining within the range reported by Wang et al. (2018) for the peatlands in the PMFB.

It is important to highlight that, even when comparing our results with other studies, these rates are derived from different types of measurements or approaches. For example, Lähteenoja et al. (2009) reports apparent carbon accumulation rate (ACAR) values based on radiocarbon dating, while Wang et al. (2018) present averages from simulations across several sites in PMFB. As Young et al. (2021) concluded, the ACAR and the Net Carbon Balance (NCB) exhibit opposite behaviours in long-term analyses, leading to mismatches in the estimated magnitude of NCB. The same distinction applies to peat accumulation rates; however, when considering the full history of a peatland, it is possible to compare some of these rates on average Frolking et al. (2014).

In comparison with other simulations for tropical peatlands worldwide, Peruvian Peatlands appear to exhibit similar or higher carbon accumulation rates (Table 3). This may be attributed to the Peruvian Amazon being one of the wettest environments, with higher precipitation Garcin et al. (2022); Lavado Casimiro et al. (2012), which maintains a favourable WT dynamic for peat accumulation process Evans et al. (2014); Hergoualc'h et al. (2020).

4.3 Sensitivity analysis

Between the two simulated sites, the NYO-03 (PF) is more sensitive than VEN-02 (PS), particularly with respect to changes in the initial NPP and decomposition rates. Other studies have highlighted the vulnerability of rainwater-fed ecosystems as NYO-03, particularly to drainage and hydrological disturbances Draper et al. (2018); Flores Llampazo et al. (2022); Honorio Coronado et al. (2021).

The ±25% change in precipitation did not result in substantial differences in final peat depth or total carbon. This is likely explained by the high precipitation levels in the Peruvian Amazon. Peat accumulation, therefore, appears to be more strongly influenced by local ecological factors such as river migration, sedimentation, and topography configuration Roucoux et al. (2013); Wang et al. (2022); Lawson et al. (2026). VEN-02 seems less sensitive than NYO-03 to precipitation variation, possibly because VEN-02 is more strongly influenced by river dynamics, whereas NYO-03 is classified as a rain-fed ecosystem.

From an ecosystem perspective, PF and OP appear to be the most sensitive EcoTy (Appendix B Figure B4). PF is generally more stable in terms of hydrology, more isolated in both topographic and hydrological connectivity, and characterised by thinner-stemmed vegetation. In contrast, OP is associated with non-vascular vegetation and exposed to wider WT fluctuations. These factors likely explain the high sensitivity observed in both ecosystems in the simulation Bourgeau-Chavez et al. (2021); Flores Llampazo et al. (2022); Honorio Coronado et al. (2021); Lähteenoja et al. (2011). In the Peruvian Amazon, the peat accumulation appears to be strongly influenced by productivity and decomposition rates, which may be altered by local activities such as palm harvesting Hergoualc'h et al. (2017); Hidalgo Pizango et al. (2022).

When the precipitation was altered by +30 to +45% the changes in final peat depth were minor (Appendix B Figure B5). Although our simulation was not sensitive to an increase in precipitation, Flores Llampazo et al. (2022) highlight the consequences of extreme flooding events in all EcoTy. The lack of sensitivity in our model may be related to the simplified model used to recreate WT fluctuations, which constrains water dynamics to belowground, and does not include inundation associ-

https://doi.org/10.5194/egusphere-2026-2272
Preprint. Discussion started: 29 April 2026

ated with river floodplains. In contrast, decreases in precipitation (drought events) produced substantial changes in both sites, particularly in NYO-03.

Bottino et al. (2024) warned that land-use and climate change could reduce annual precipitation by up to 44% if the Amazon transitions into savanna, while Hajdu et al. (2025) emphasised the risk of "savannisation" of the Amazon under the current deforestation rate. Both studies suggest that the future precipitation reduction, combined with a longer dry season and more extreme drought events in Amazonia, would be a critical scenario particularly for PF ecosystems, where a 45% decrease in precipitation resulted in more than 50% reduction in final peat depth (Appendix B Figure B6). Further evidence of PF vulnerability comes from the study by dos Reis et al. (2021), which reported that in the Amazon, the thickest-stemmed trees are the most resistant to drought periods. Since PF are characterised by a thinner-stemmed forest, they are expected to be more sensitive.

Garcin et al. (2022) highlighted that the current precipitation in central Congo (1,400 mm y^{-1}) could be approaching drought threshold that limits peat accumulation. In the western Amazon a 45% reduction corresponds to roughly 1,650 mm y^{-1}, both precipitations appear similar in terms of critical threshold for detrimental effects on peat accumulation. Furthermore, this reduction in precipitation also falls within the established critical threshold and safe boundary for Amazon resilience reported by Flores et al. (2024).

4.4 Model limitations:

In this study, its application to the Peruvian Amazon required incorporating a period-based approach supported by palaeoecological analysis. Simulating by periods, which represent the site's evolution as a dynamic ecosystem, provides flexibility by allowing the use of different parameters set for each EcoTy. However, this approach relies on the assumption that present-day EcoTy shares similar parameters with those that existed in the past. Furthermore, we assume the timing of shifts between EcoTy based on the pollen matrix. What caused these EcoTy transitions? In our model the shifts are forcing as the climate data. Incorporating dynamic shifts within HPMTrop would require substantial model development, guided by the hypothesis that the EcoTy shifts in Peruvian Amazon peatlands, at least during the Holocene, appear to be more strongly influenced with local factors such as river migration more than climatic drivers. This pattern may be different from that observed in other tropical peatlands (e.g., Congo Basin) or the northern peatlands. Additionally, improved regional climate reconstructions are needed, including the climatic variability across different time scales.

Several parameters in HPMtrop applied to the Peruvian Amazon were obtained by EcoTy, defined as a range of plausible values within each ecosystem. The initial values were derived from literature and from linear and non-linear models using published data. Among the ecosystems, OP had the least information available for parametrisation; therefore, its values were tuned, while maintaining ranges between SFF and PS, which are the most closely related ecosystems to OP within Peruvian peatlands. Despite the limitations and simplicity of the models used to represent physical processes in the Peruvian Amazon, the integration of peat core information, pollen analysis and model simulation, provided valuable insights into how peat accumulation dynamics occur in this region. Such integration helps in understanding tipping points, such as the shift between

https://doi.org/10.5194/egusphere-2026-2272
Preprint. Discussion started: 29 April 2026

ecosystem types, which are often associated with changes in water table fluctuations and vegetation dominance, determining differences in peat accumulation rates and whether ecosystems function as carbon sinks or sources.

Precipitation is the driver variable in the model; however, when increased the response by site and EcoTy did not show substantial changes. This may be explained by two main factors: first, the high levels of precipitation in the western Amazonian (3,000 mm y^{-1}), and second Holocene-scale precipitation reconstructions are weak and uncertain along with the limited evapotranspiration, which was simplified to a fixed scalar of 100 mm per month. Although this value of evapotranspiration is supported by several studies as an average for tropical forest, it remains a key parameter that should be improved and incorporated as a variable.

Transition periods were represented as linear, gradual changes between EcoTy, which constituted a limitation. This simplification produces chaotic outputs during transition periods, resulting in some cases in outliers. Transition periods require specific verification and validation. However, even palaecological approaches have limitations in identifying the exact timing of shifts between ecosystems.

The simulations in all cases showed substantial increase in final peat depth when either NPP was increased or base decomposition rate was decreased. This response likely reflects a structural bias in the model rather than an inherent ecological sensitivity, as HPMTrop is highly responsive to those initial values. A further remaining questions and points of discussion are described in the Appendix B Text B2.

5 Conclusions

HPMtrop_EcoTy produces a remarkably good age-depth profile compared with the reference cruves from the cores. This does not necessarily mean the model is fully correct, since parameter tuning was involved, but it does indicate that the model provides a plausible hypothesis for the development of these peat deposits. The model could also reveal the consequences for the net carbon balance, which would include long intervals of net carbon loss in the two different EcoTy in the Peruvian Amazon. It is worth noting that transitions between EcoTy lead to either an increase or decrease in peat and carbon accumulation rates. Transitions from wetter to drier conditions (e.g., PS to SFF), resulted in a negative transition characterised by peat and carbon loss. After an extensive period of deep-water table (SFF), the transition back to a peat-forming ecosystem (PS) resulted in a positive peat accumulation rate but a negative carbon accumulation rate, indicating that even under wetting conditions, the decomposition of older peat can continue, producing a delayed effect that drives a negative carbon balance. The most sensitive ecosystem was the Pole Forest (NYO-03 site) and Open peatlands, where changes in either NPP or decomposition rate generated a more pronounced effect on final peat and carbon accumulation than changes in precipitation. The processes that drive peat accumulation in Peruvian Amazon peatlands appear to be more dependent on local ecological factors, such as river migration, which may trigger the shift between EcoTy, and may be different to the other tropical peatlands such as in the Congo basin where the precipitation was more important.

https://doi.org/10.5194/egusphere-2026-2272
Preprint. Discussion started: 29 April 2026

Table 2. Definition of range of periods and the corresponding EcoTy by site

Site	Period cal. yr BP (EcoTy)	Δ peat accumulation rate (mm y^{-1})	Peat height (m)	Δ Carbon (g C m^{-2} y^{-1})	Vegetation dominance (from pollen)	NPP (kg C m^{-2} y^{-1})	Decomposition (kg C m^{-2} y^{-1})	WT (cm)
NY0-03	4917-6175 (PS)	0.82	1.02	38.96	*Mauritiella*	0.70	0.59	0.03
	4147-4917 (PS to SFF)	-0.28	0.81	-4.71		0.92	0.92	0.16
	1646-4147 (SFF**)	0.06	0.96	3.76	*Symmeria*	0.89	0.89	0.3
	1436-1646 (SFF to PS)	0.27	1.01	-15.50		0.78	0.80	0.06
	216-1436 (PS)	2.26	3.77	96.17	*Mauritia*	0.70	0.61	0.03
	166-216 (PS to PF)	11.3	4.33	31.66		0.57	0.54	0.02
	0-166 (PF)	1.33	4.56	56.75	*Pachira*	0.58	0.52	0.003
VEN-02	946-1129 (OP*)	4.48	0.82	177.18	*grasses*	1.01	0.83	0.03
	589-946 (OP to PS)	0.11	0.85	27.19		0.85	0.82	0.03
	0-589 (PS)	0.55	1.18	24.33	*Mauritia*	0.70	0.68	0.03
Sim NYO-03	**6175**(3 EcoTy)	**0.70**	**4.56**	**29.13**	**Veg**	**0.81**	**0.76**	**0.16**
Sim VEN-02	**1129**(2 EcoTy)	**1.04**	**1.18**	**49.89**	**Veg**	**0.80**	**0.75**	**0.03**

* OP water table dynamics were modelled using the same relationship as for PS due to lack of ground data. ** SFF shows a hiatus period with very low peat accumulation over more than 2000 years. *Note:*: Type of ecosystem (EcoTy), Pole Forest (PF), Palm Swamp (PS), Seasonal Flooded Forest (SFF), Open Peatland (OP), water table (WT). Δ Carbon is the carbon accumulation rate in g C m^{-2} y^{-1}. Simulation (Sim) NYO-03 and VEN-02 represent the average peat and carbon accumulation rate over the entire simulation period at each site (average across all EcoTy including TP).

https://doi.org/10.5194/egusphere-2026-2272
Preprint. Discussion started: 29 April 2026

Table 3. Simulated carbon accumulation rates for the Peruvian Amazon compared with other tropical peatlands worldwide. The carbon accumulation rates are expressed in g C m^{-2} y^{-1}.

Tropical peatland	Carbon accumulation rate	Model	Study
Congo	25	Digibog_Congo	Young et al. (2021)
Southeast Asia	30	HPMTrop	Kurnianto et al. (2014)
Peruvian Amazon (NYO-03)	49.9	HPMTrop_EcoTy	This study
Peruvian Amazon (VEN-02)	29.1	HPMTrop_EcoTy	This study

Note: Net primary productivity (NPP) simulated output for different plant components and ecosystem types (EcoTy). PF: Pole Forest; PS: Palm Swamp; SFF: Seasonal Flooded Forest; OP: Open Peatland. AG: aboveground; BG: belowground. For SFF, the PalmsAG and PalmsBG components are not considered within the model (0). For OP, only grass components are considered, with aboveground represented by leaves and belowground by roots.

https://doi.org/10.5194/egusphere-2026-2272
Preprint. Discussion started: 29 April 2026

Code and data availability. The data, sources and the code used in this study are stored in public repository: Puerta, Y. T., et al. (2026). Zenodo with doi: 10.5281/zenodo.18713887 (https://shorturl.at/dgBoZ). The original paper that described the model is Frolking et al. (2010).

Appendix A: Parameters

A1 Bias correction of precipitation forcing

To reduce the systematic bias in the precipitation values used as forcing in the HPMTrop model, a bias correction was applied using observed precipitation data from ground stations Bagazan, Santa Rita and Nauta from de Meteorología e Hidrología del Perú (SENAMHI). Approximately 10 years of stations record was used to calculate a mean monthly precipitation for each month (January to December). Monthly bias-correction factor was calculated as the ration between the observed mean monthly precipitation and the corresponding mean monthly precipitation simulated by CCSM3. As a result one bias-correction factor for each month was obtained and applied multiplicatively to the entire precipitation time series used as forcing in the model. Each month value was scaled by the corresponding bias-correction factor. The bias-corrected precipitation time series preserve the long-term temporal variability and the trends of the original precipitation time series simulated by CCSM3 TraCE-21ka but with adjusted of seasonal precipitation mean values closer to the observed precipitation.

$$P_{corrected(t)} = P_{simulated(t)} \times \frac{\bar{P}_{observed(m)}}{\bar{P}_{simulated(m)}}$$

Where P is the precipitation (mm), t is the time step, m is the month (1 to 12), $\bar{P}_{observed(m)}$ is the mean observed precipitation for month m, and $\bar{P}_{simulated(m)}$ is the mean precipitation for month m simulated by CCSM3.

https://doi.org/10.5194/egusphere-2026-2272
Preprint. Discussion started: 29 April 2026

Table A1. NPP by plant component and EcoTy

EcoTy	Component	NPP (kg m^{-2} $month^{-1}$)	Source
PF	Leaves	0.080	Dargie et al. (2024)
PF	Stem	0.014	Dargie et al. (2024)
PF	Root	0.003	Dargie et al. (2024)
PF	PalmsAG	0.017	Dargie et al. (2024)
PF	PalmsBG	0.014	Dargie et al. (2024)
PS	Leaves	0.014	Dargie et al. (2024)
PS	Stem	0.003	Dargie et al. (2024)
PS	Root	0.001	Dargie et al. (2024)
PS	PalmsAG	0.066	Dargie et al. (2024)
PS	PalmsBG	0.082	Dargie et al. (2024)
SFF	Leaves	0.111	del Aguila-Pasquel et al. (2013)
SFF	Stem	0.046	del Aguila-Pasquel et al. (2013)
SFF	Root	0.068	del Aguila-Pasquel et al. (2013)
SFF	PalmsAG	NA	
SFF	PalmsBG	NA	
OP	Leaves	0.105	Basuki et al. (2021)
OP	Stem	NA	
OP	Root	0.087	Basuki et al. (2021)
OP	PalmsAG	NA	
OP	PalmsBG	NA	

Net primary productivity (NPP) values obtained from the literature for each ecosystem type (EcoTy) used within the model. PF: Pole Forest; PS: Palm Swamp; SFF: Seasonal Flooded Forest; OP: Open Peatland. AG: aboveground; BG: belowground. For SFF, the PalmsAG and PalmsBG components are not considered within the model (NA). For OP, only grass components are considered, with aboveground represented by leaves and belowground by roots.

https://doi.org/10.5194/egusphere-2026-2272
Preprint. Discussion started: 29 April 2026

Table A2. Decomposition values by EcoTy

EcoTy	Component	K (month^{-1})	Source
PF	Leaves	0.064	Hergoualc'h et al. (2023)
PF	Stem	0.011	Dargie et al. (2024)
PF	Root	0.030	Dezzeo et al. (2021)
PF	PalmsAG	0.134	Dargie et al. (2024)
PF	PalmsBG	0.016	Dargie et al. (2024)
PS	Leaves	0.064	Hergoualc'h et al. (2023)
PS	Stem	0.011	Dargie et al. (2024)
PS	Root	0.030	Dezzeo et al. (2021)
PS	PalmsAG	0.145	Dargie et al. (2024)
PS	PalmsBG	0.020	Dargie et al. (2024)
SFF	Leaves	0.180	Capps et al. (2011)
SFF	Stem	0.050	Martins et al. (2023)
SFF	Root	0.115	Violita et al. (2016)
SFF	PalmsAG	NA	
SFF	PalmsBG	NA	
OP	Leaves	0.033	Wright et al. (2013)
OP	Stem	NA	
OP	Root	0.073	Snyder and Rejmánková (2015)
OP	PalmsAG	NA	
OP	PalmsBG	NA	

Exponential decomposition values (k) for different plant components and ecosystem types (EcoTy) used within the model. PF: Pole Forest; PS: Palm Swamp; SFF: Seasonal Flooded Forest; OP: Open Peatland. AG: aboveground; BG: belowground. For SFF, the PalmsAG and PalmsBG components are not considered within the model (NA). For OP, only grass components are considered, with aboveground represented by leaves and belowground by roots.

https://doi.org/10.5194/egusphere-2026-2272
Preprint. Discussion started: 29 April 2026

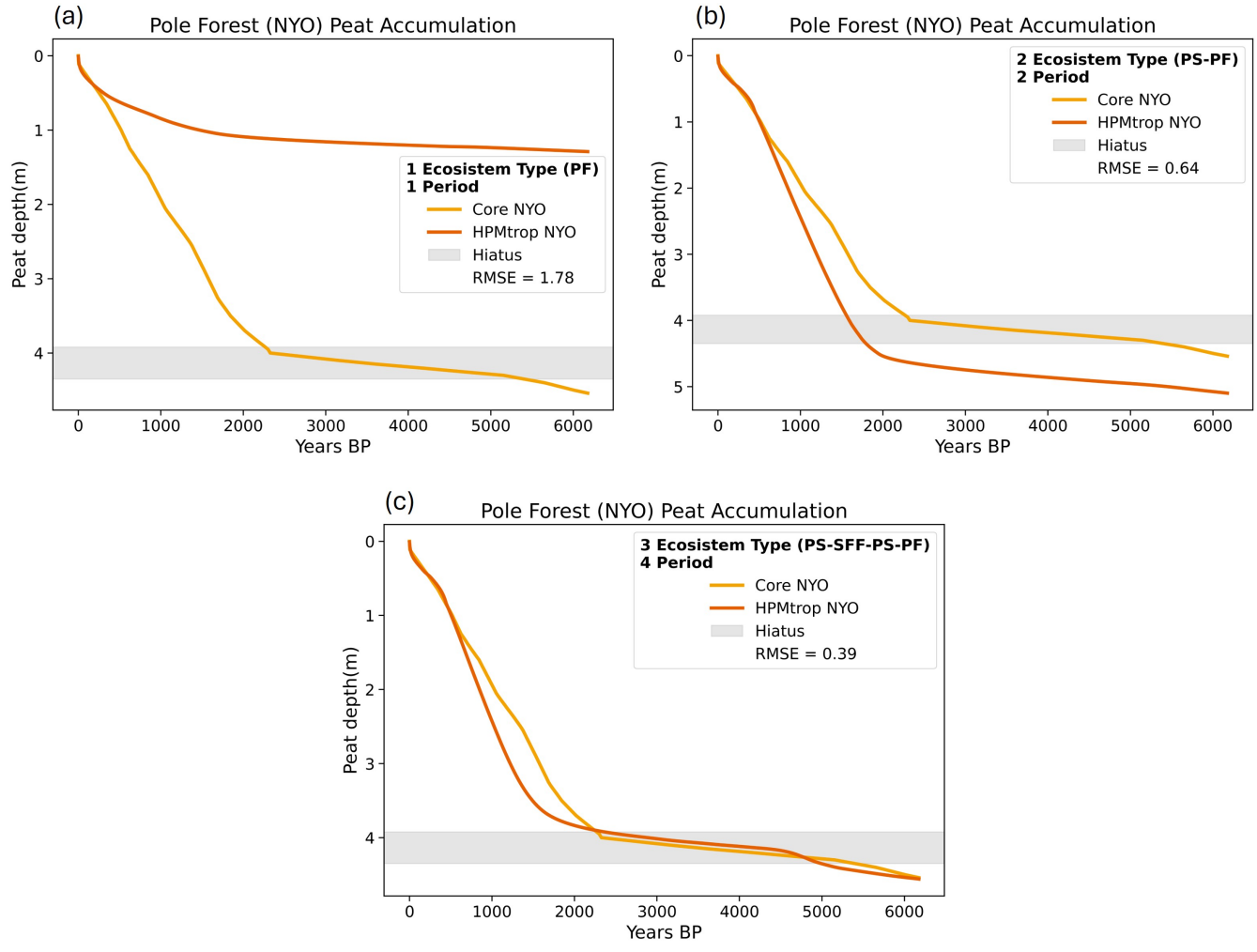

Figure A1. Evolution of the simulation for the Nueva York site (NYO-03) under scenarios in which new ecosystem types (EcoTy) were introduced during specific time intervals. The yellow line represents the site core, and the orange line represents the simulated curve. (a) Simulation considering only Pole Forest (PF) for approximately 6,000 years BP. (b) Simulation in which Palm Swamp (PS) is included during the first 4,000 years of the simulation (between 6,000 and 2,000 years BP), followed by PF during the last 2,000 years. (c) Simulation in which the first ∼1,000 years correspond to PS, the following ∼2,500 years (approximately between 4,000 and 1,600 years BP) correspond to Seasonal Flooded Forest (SFF), and PS and PF dominate during the last 2,000 years BP, with PF introduced only during the last 166 years BP.

https://doi.org/10.5194/egusphere-2026-2272
Preprint. Discussion started: 29 April 2026

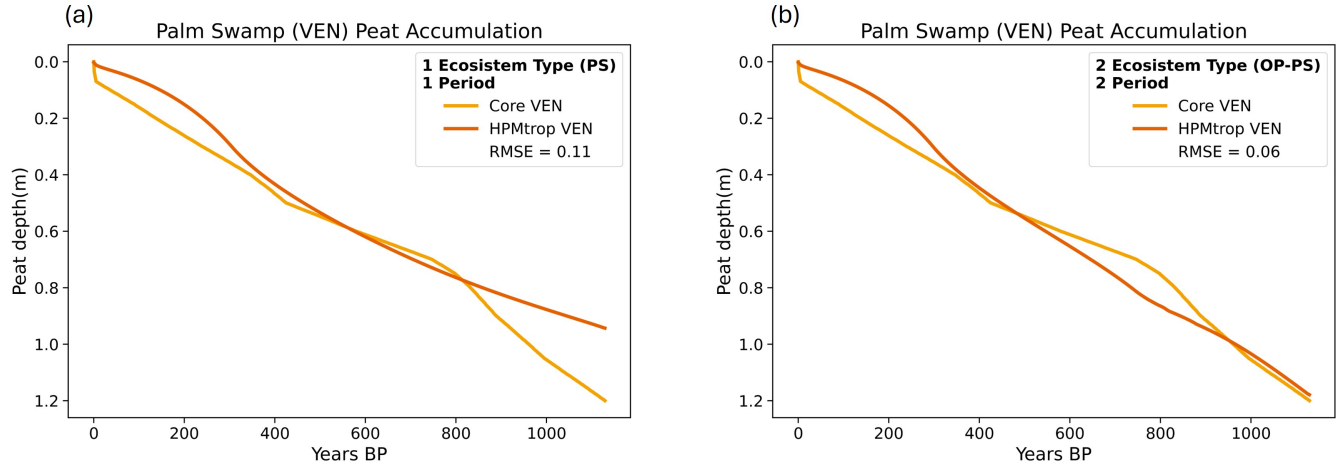

Figure A2. Evolution of the simulation for the Veinte de Enero site (VEN-02) under scenarios in which new ecosystem types (EcoTy) were introduced during specific time intervals. The yellow line represents the site core, and the orange line represents the simulated curve. (a) Simulation considering only Palm Swamp (PS) ecosystem during the entire 1,129 years of the simulation. (b) Simulation in which the first half of the time correspond to open peatlands (OP) ecosystem, and the other half of the simulation to PS ecosystem.

https://doi.org/10.5194/egusphere-2026-2272
Preprint. Discussion started: 29 April 2026

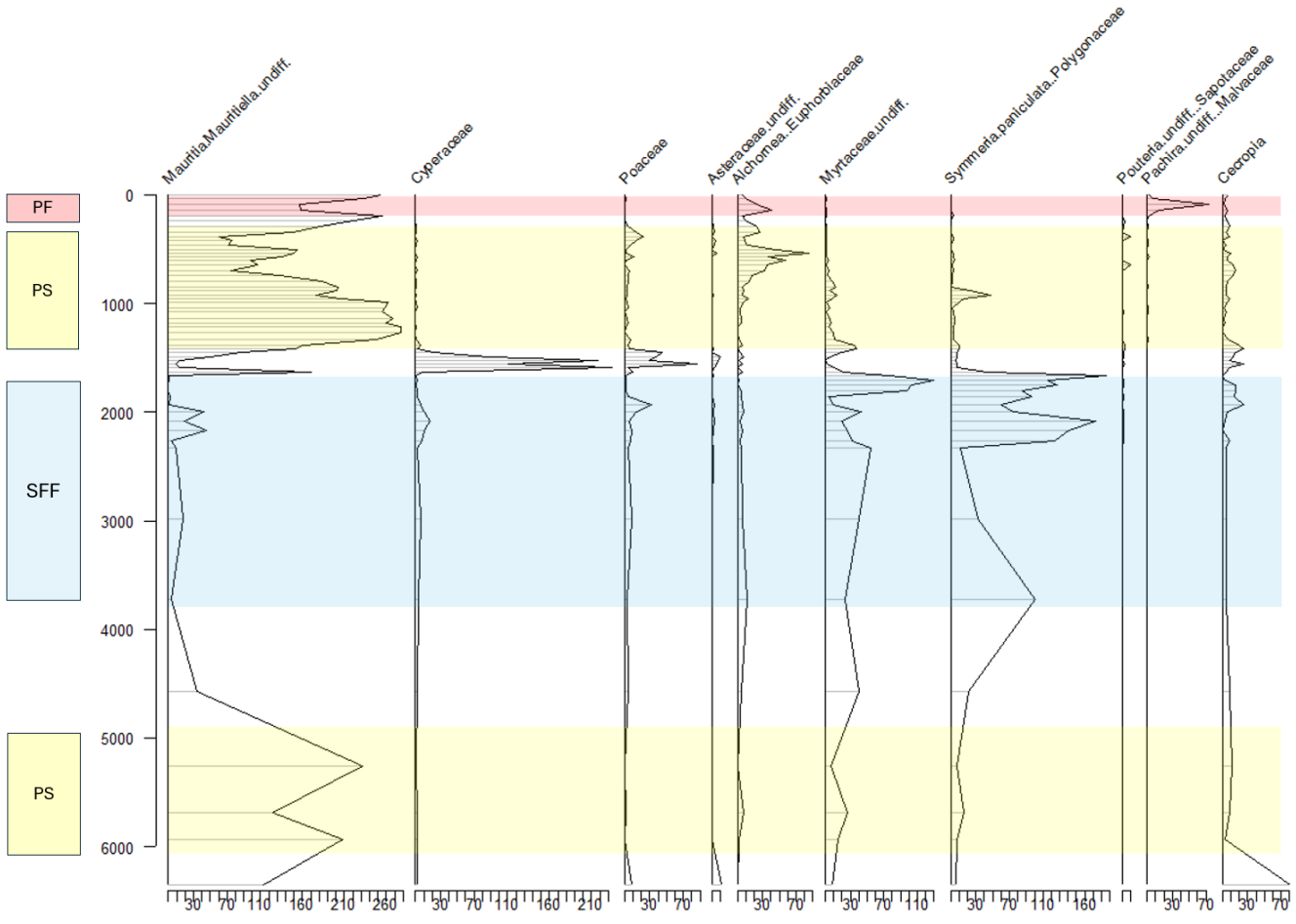

Figure A3. Pollen diagram summarising the pollen data used to define the time intervals selected from the NYO-03 site for simulations with the corresponding ecosystem types (EcoTy). Data from *Åkesson et al., in prep.*. Colours indicate the different EcoTy as follows: pale red, Pole Forest (PF); pale yellow, Palm Swamp (PS); and pale blue, Seasonal Flooded Forest (SFF).

https://doi.org/10.5194/egusphere-2026-2272
Preprint. Discussion started: 29 April 2026

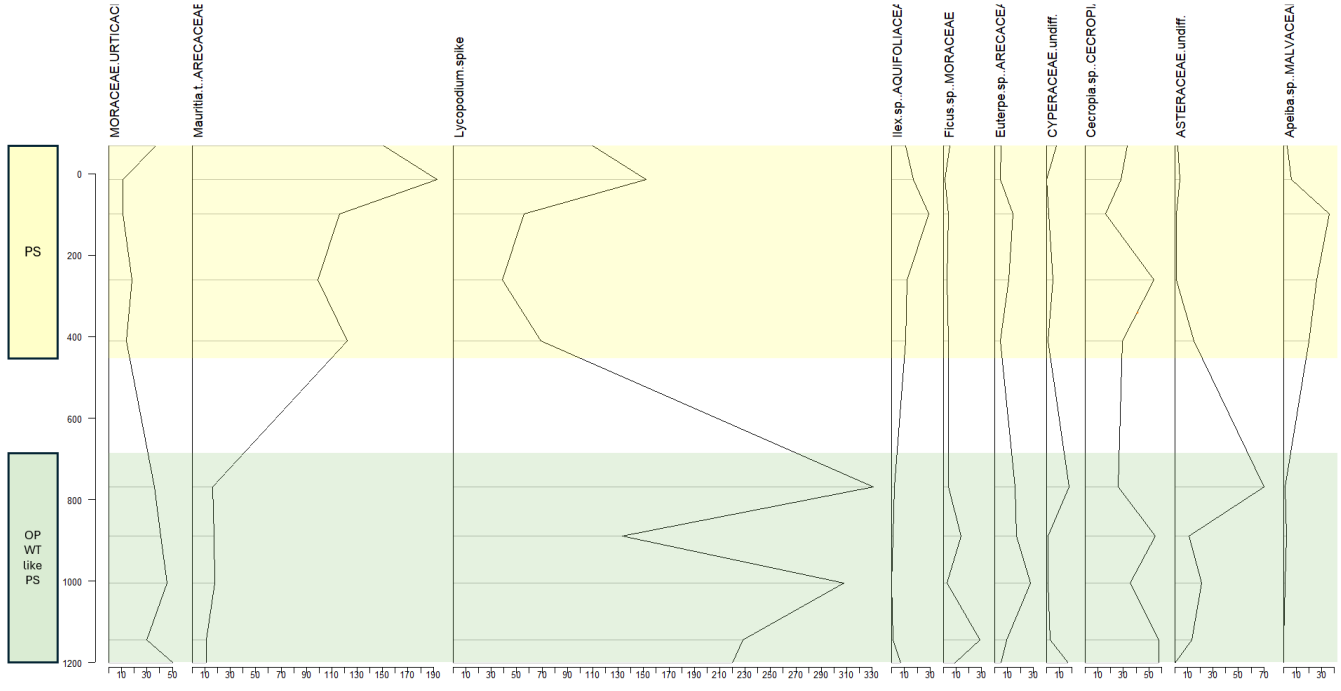

Figure A4. Pollen diagram summarising the pollen data used to define the time intervals selected from the VEN-02 site for simulations with the corresponding ecosystem types (EcoTy). Data from *Akesson in prep*. Colours indicate the different EcoTy as follows: pale yellow, Palm Swamp (PS) and pale green, open peatlands (OP).

https://doi.org/10.5194/egusphere-2026-2272
Preprint. Discussion started: 29 April 2026

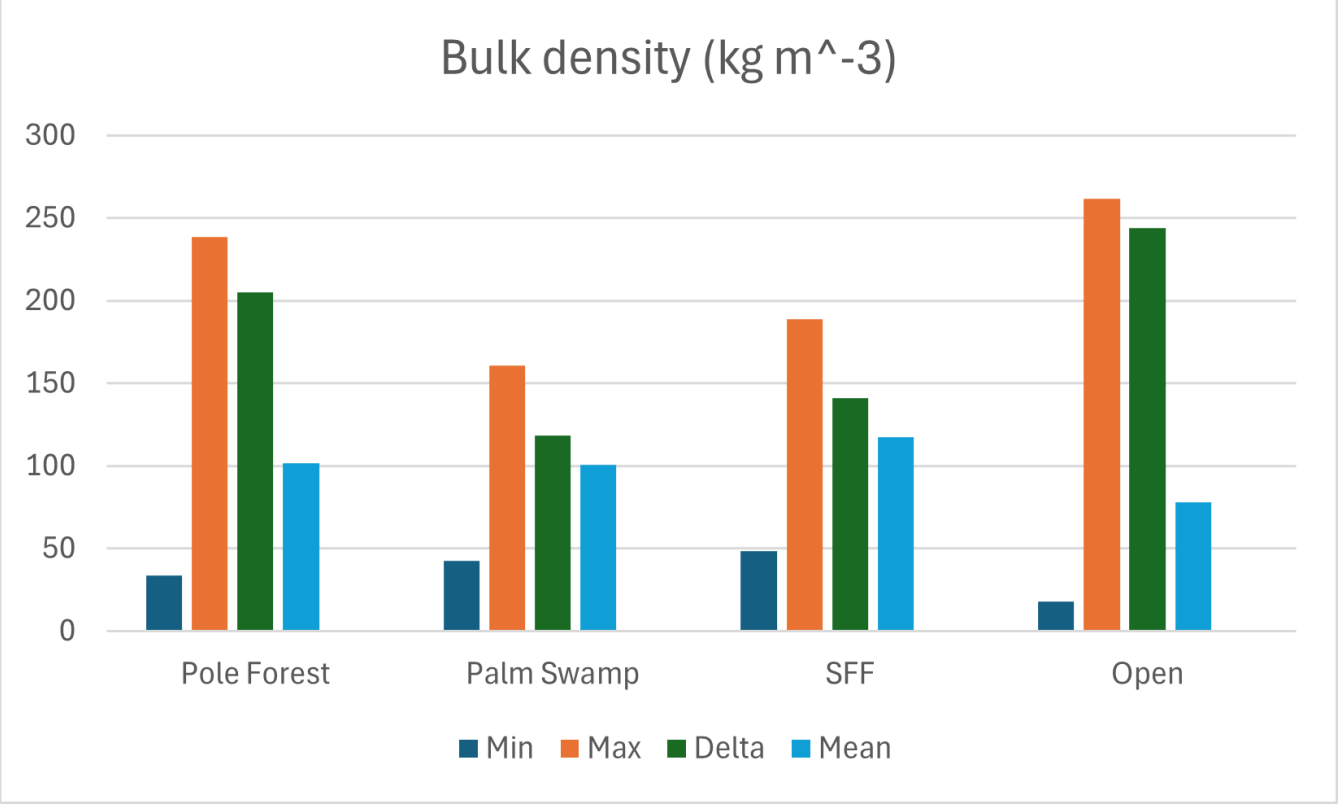

Figure A5. Bulk density (BD) values for different ecosystem types (EcoTys) used within the model. PF: Pole Forest; PS: Palm Swamp; SFF: Seasonal Flooded Forest; OP: Open Peatland. The bar plot shows basic statistics, including minimum BD (min), maximum BD (max), delta BD (Delta), and mean BD (mean). These BD values were calculated from a database compiled from different sources reporting BD values in Peruvian peatlands Lähteenoja et al. (2009, 2011); Kelly; Honorio Coronado et al. (2021).

https://doi.org/10.5194/egusphere-2026-2272
Preprint. Discussion started: 29 April 2026

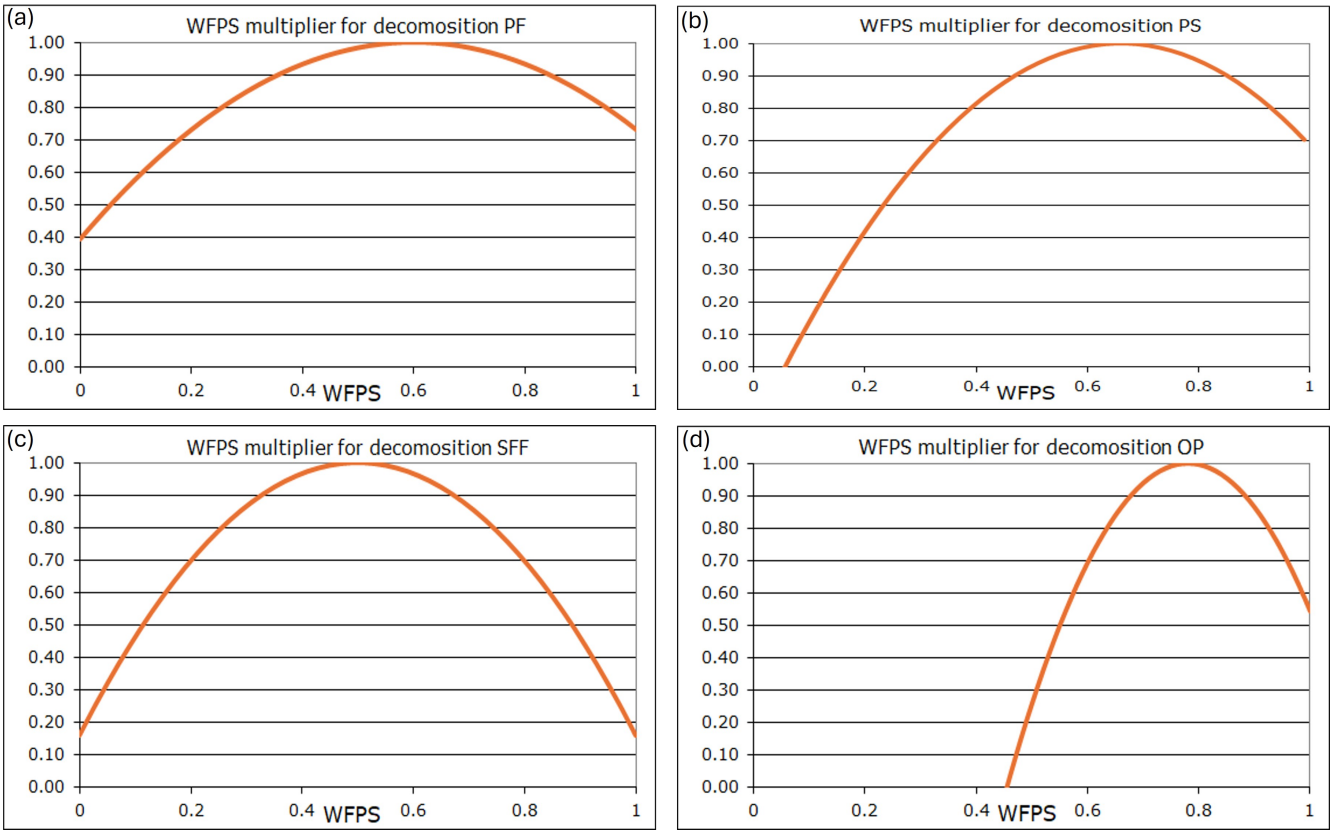

Figure A6. Water-filled pore space model developed to obtain soil properties, including minimum, optimum, and maximum saturation rates, and field capacity, used as parameters within the model for each ecosystem type (EcoTy). The values used to construct the curves were obtained from literature sources reporting soil properties in Peruvian peatlands (Hergoualc'h et al. (2023, 2020); Fonseca et al. (2019); Bruno et al. (2006); Hodnett et al. (1995); Moyano et al. (2013)). (a) Pole Forest (PF). (b) Palm Swamp (PS). (c) Seasonal Flooded Forest (SFF). (d) Open Peatland (OP).

https://doi.org/10.5194/egusphere-2026-2272
Preprint. Discussion started: 29 April 2026

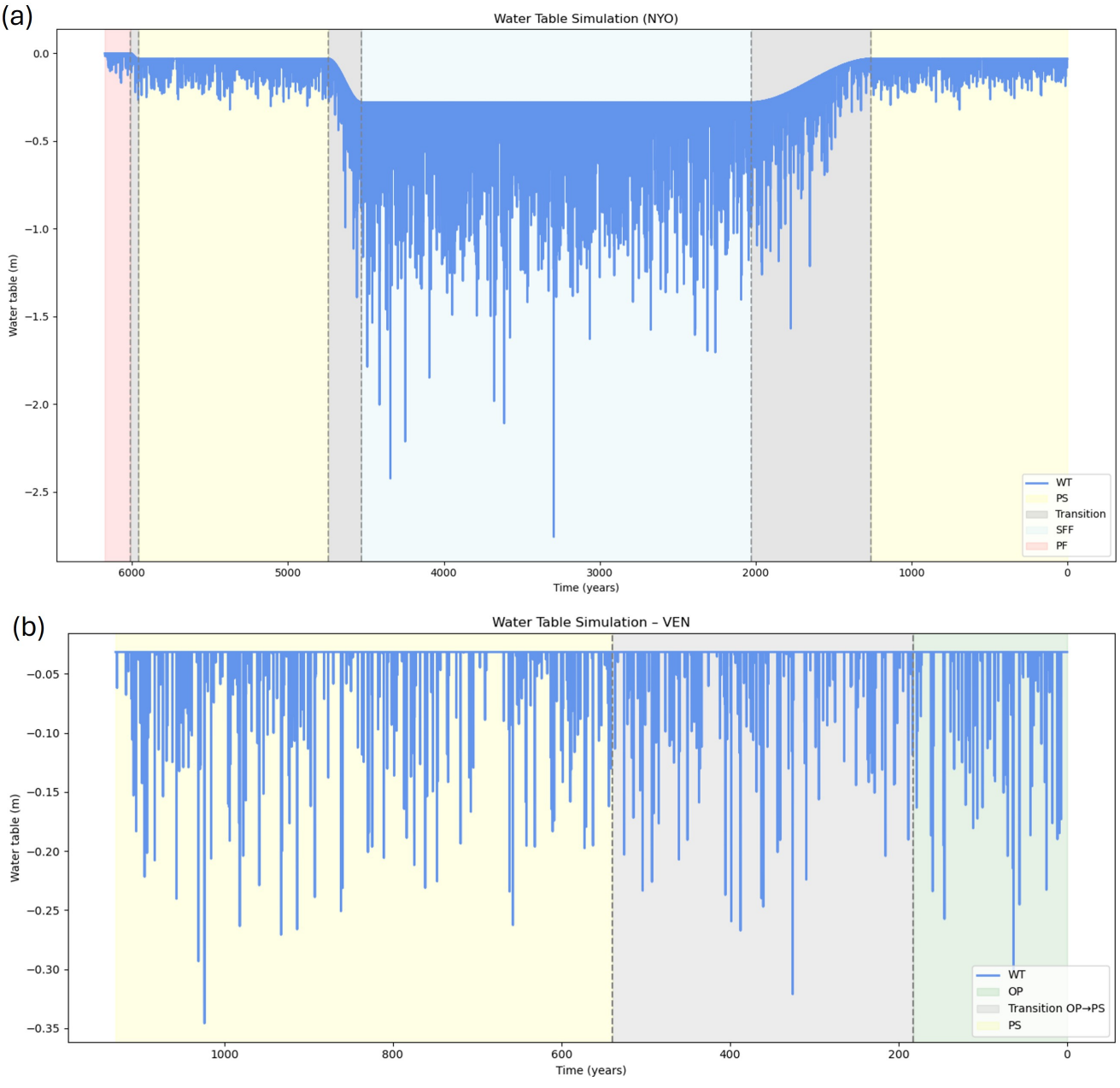

Figure A7. Water table (WT) values simulated by the model for each ecosystem type (EcoTy). PF: Pole Forest; PS: Palm Swamp; SFF: Seasonal Flooded Forest; OP: Open Peatland. The plots show WT simulations for the Nueva York-03 (NYO-03) and Veinte de Enero-02 (VEN-02) sites. (a) NYO-03 WT reconstruction for the entire simulation period. (b) VEN-02 WT reconstruction for the entire simulation period. (c) Seasonal Flooded Forest (SFF)

https://doi.org/10.5194/egusphere-2026-2272
Preprint. Discussion started: 29 April 2026

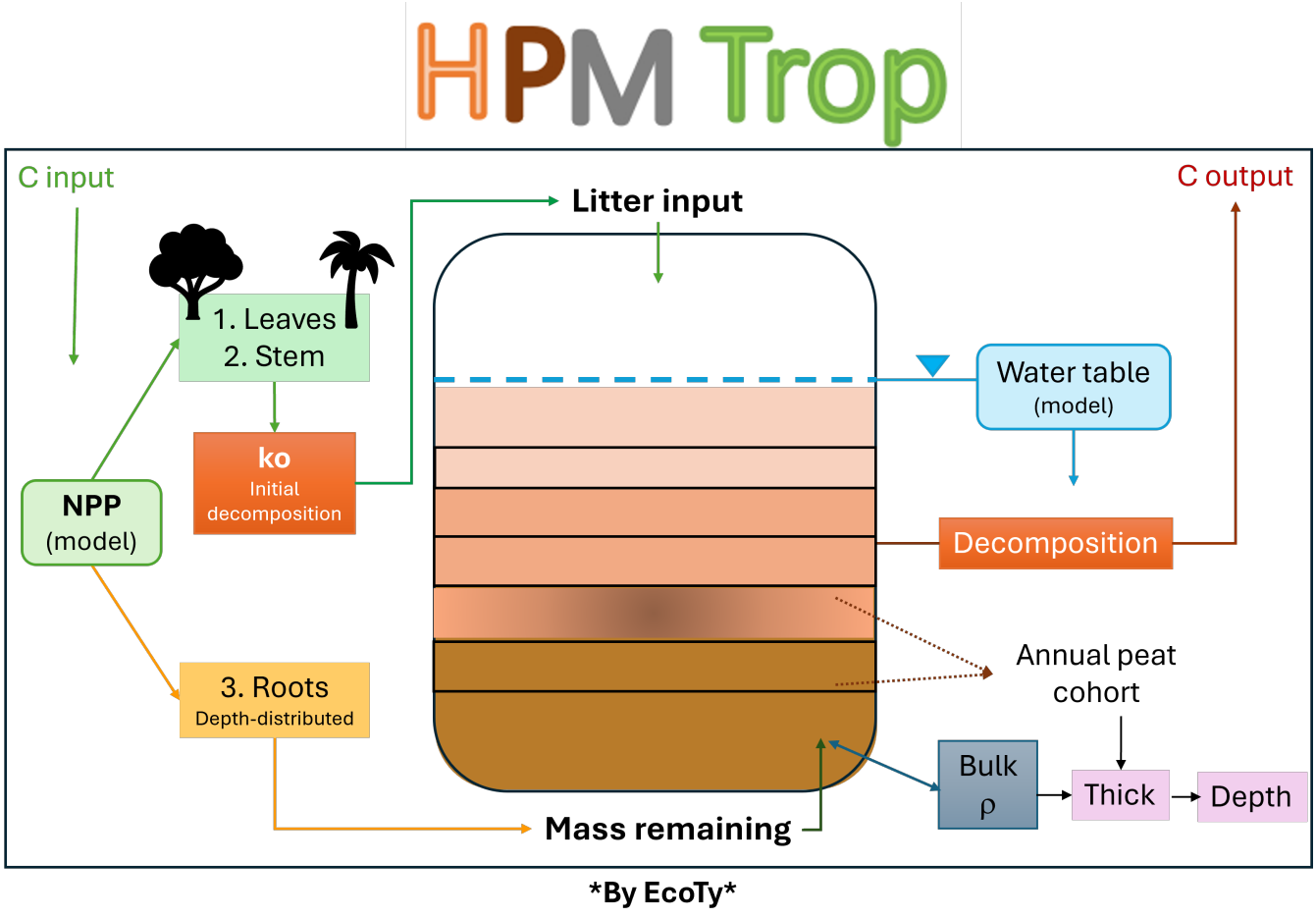

Figure A8. HPMTrop_EcoTy applied for Peruvian peatland sites in Amazonia. Conceptual representation of the main process in HPMTrop model to drive the peat accumulation dynamics. These processes are mediated by ecosystem type (EcoTy), meaning the model takes into account the ecological history and ecosystem-specific parameters to represent peat accumulation over time at a given site. Carbon (C). A net primary productivity (NPP) model. Initial decomposition values (Ko) for each plant component. Bulk density (ρ)

Appendix B: Results and discussion

B1 Sensitivity analysis by EcoTy

The ecosystems show greater sensitivity response to increases or decreases NPP. PF and OP exhibited the largest changes in peat height across the entire simulation. At the VEN-02 site in the base simulation, peat height for OP reached 0.8 m (946 y BP). When NPP was increased and decrease by 25% peat height changed 77% and 44% respectively during the OP period. At NYO-03 site, during the PF period (0-166 cal. yr BP) peat height reached 4.6 m in the base simulation. When NPP was increased by 25%, peat height increased by 75%, while when NPP was decreased by 25%, peat height reduced by 48%. After

https://doi.org/10.5194/egusphere-2026-2272
Preprint. Discussion started: 29 April 2026

PF and OP, the next ecosystem with high sensitivity to changes in productivity was PS, showing 53% increase with higher NPP and 39% decrease with lower NPP; while SFF was the least sensitive.

K: Similar to NPP, changes in initial decomposition values produced strong responses at both sites and across EcoTy. The OP period at VEN-02 site showed the greatest sensitivity, when decomposition rate was increased by 25%, peat height decreased by 38%, whereas and a 25% reduction in k resulted in an increase in peat height of about 100%. At NYO-03, the PF showed an increase of more than 70% in peat height when k was decreased, and decrease of more than 30% when k was increased. The PS ecosystem produced an increased of approximately 75% in peat height at NYO-03 and more than 40% at VEN-02 under a 25% reduction in K. When k increase 25%, peat height decreased by 37% at NYO-03 and 25% at VEN-02. SFF was the least sensitive.

P: When precipitation was altered by $\pm 25\%$, the resulting changes were not substantial. In fact, it was the least sensitive parameter across both sites and all EcoTy. Despite that, PF and OP showed relatively greater sensitivity, particularly under reduced precipitation. A possible explanation for the overall low sensitivity is the high precipitation in the region (2900 mm y^{-1}). However, a general trend can be identified, all ecosystems were more sensitive to decrease in precipitation than to increase. For this reason, a more detailed sensitivity exploration of precipitation sensitivity was conducted to identify potential tipping points.

B2 Remaining questions and future research:

After adapting, applying HPMTrop, and reviewing long-term peat accumulation models such as DIGIbog and Mpeat, a reflection arises: although mathematical models and specific constraints could be good enough to gain insights about Amazon tropical peatlands, they should be regarded primarily as a first step. For instance, in Amazon peatlands, an appropriate model should incorporate river migration dynamics, a crucial factor influencing peat accumulation processes. Similarly, integrating palaeoecological knowledge would improve understanding of how peat accumulation has occurred over time. Peatland modelling is inherently interdisciplinary, offering a holistic framework that helps place each ecological piece into the large puzzle of peat formation processes. However, significant data gaps remain, particularly regarding reliable parameterisation to represent the complex physical process governing the Amazon Tropical peatland.

Even with the same ecosystem classification (e.g., PS, PF), applying fixed parameters may not adequately represent conditions at a specific site. Peatland ecosystem evolution depends strongly on in situ factors, which can vary considerably even among sites classified as the same ecosystem type. Peatland formation can be understood as a state-dependent system influenced by both past and present conditions, and it is possible for the same ecosystem type to develop alternative stable states under a set of environmental conditions. For example, soil properties may be shaped by localised processes such as deposition, erosion, water table dynamics, river migration and plant response (Beisner). Even similar ecosystems (or the same ecosystem type) may exhibit emerging properties as a result of local and endogenic processes and site-specific perturbations. This means that the site retains a distinctive character, shaped by the historical trajectory of evolution, a process that is neither linear nor

https://doi.org/10.5194/egusphere-2026-2272
Preprint. Discussion started: 29 April 2026

standardised. In this sense, a peatland site may be thought of as a "fingerprint", reflecting the diverse configuration of driving factors such as sediment deposition and river migration that converge to produce a specific state (Lähteenoja et al. (2011)).

Under the hypothesis that the natural shifts between EcoTy leads to loss or gain of carbon, it is natural that these ecosystems can act as either a carbon sink or source. What happens with this carbon when the ecosystem is acting as a carbon source, is it released directly into the atmosphere (CO2, CH4), or is the primary pathway through dissolved organic carbon (DOC)? This question should be addressed in a complex dynamic model (ORCHIDEE or JULES) different to HPMtrop that only simulates peat mass balance. River water sampling could provide valuable clues to address this question. As a potential hypothesis, we suggest that most of the carbon is likely lost through lateral fluxes, since water table fluctuation could transport this carbon into the rivers (Dean et al. (2025)). For example, one of the rivers associated with our ombrotrophic site (NYO-03: PF) is the Tigre River, a black water tributary of the Marañón River. This could be an indication of a nutrient limited environment and indeed this is confirmed by previous elemental analysis conducted at the site by Lähteenoja et al. (2011). Conversely, our minerotrophic site (VEN-02: PS) is associated with the Marañón River, a main tributary of the Amazon, with white water, which could indicate higher nutrient conditions and higher relative pH.

While chemical factors are not directly represented in the model, they are indirectly accounted by each EcoTy through the WT variation, the base decomposition rate parameter (K), and the soil properties parameters. For example, the minimum decomposition rate for PF was the lowest value (slow ramp-up) consistent with more stable WT conditions and saturated soil. This ecosystem exhibits greater anaerobic tolerance (Similar to reported by Hergoualc'h et al. (2020) for Intact hummocks) than PS or OP. On the other hand, PS has a low to moderate range of minimum decomposition rate, whereas OP and SFF exhibit moderate to high values. SFF is characterised by relatively rapid oxygen depletion under saturated conditions and rapid decomposition under drier conditions associated with its natural Flood-drought cycles (Cui et al. (2024); Cusack et al. (2023)). Incorporate chemical components in a long-term peat modelling could enhance the estimation of parameters associated with soil properties.

https://doi.org/10.5194/egusphere-2026-2272
Preprint. Discussion started: 29 April 2026

Table B1. Simulation NPP by plant component and EcoTy

EcoTy	npp_Leaves	npp_Wood	npp_Roots	npp_PalmsAG	npp_PalmsBG	Total_NPP
OP	5.55	0.00	4.58	0.00	0.00	**10.19**
PF	3.63	0.63	0.14	0.77	0.63	**5.82**
PS	0.59	0.13	0.04	2.80	3.48	**7.03**
SFF	4.43	1.81	2.69	0.00	0.00	**8.94**

Net primary productivity (NPP) simulated output for different plant components and ecosystem types (EcoTy). PF: Pole Forest; PS: Palm Swamp; SFF: Seasonal Flooded Forest; OP: Open Peatland. AG: aboveground; BG: belowground. For SFF, the PalmsAG and PalmsBG components are not considered within the model (0). For OP, only grass components are considered, with aboveground represented by leaves and belowground by roots.

https://doi.org/10.5194/egusphere-2026-2272
Preprint. Discussion started: 29 April 2026

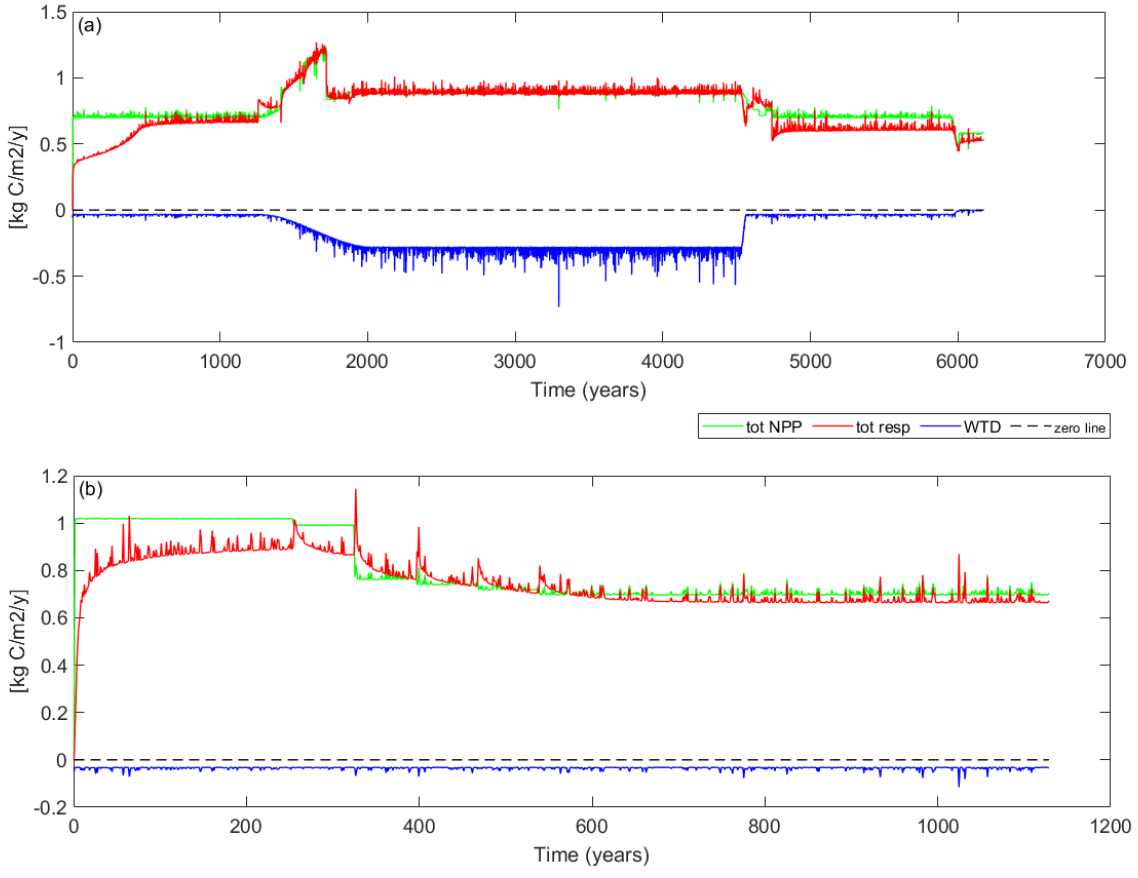

Figure B1. Net Primary Productivity (tot NPP) and respiration (tot resp) simulations for the Nueva York (NYO-03) and Veinte de Enero (VEN-02) sites, together with water table (WTD) simulations.(a) NYO-03 and (b) VEN-02 time series showing tot NPP in green, tot resp in red, and WTD simulation in blue.

https://doi.org/10.5194/egusphere-2026-2272
Preprint. Discussion started: 29 April 2026

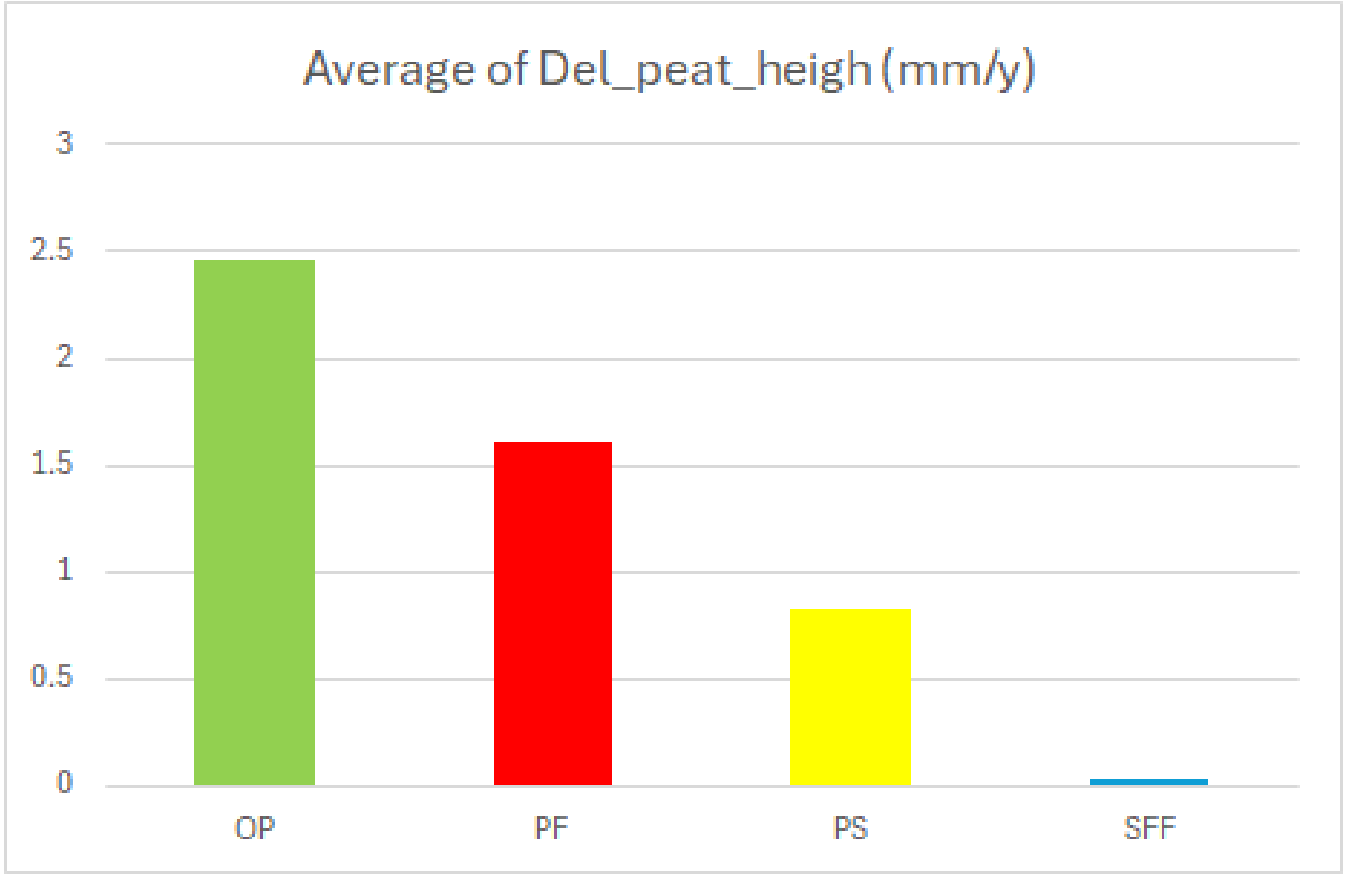

Figure B2. Peat accumulation rate simulation output from the model by ecosystem type (EcoTy). PF: Pole Forest, PS: Palm Swamp, SFF: Seasonal Flooded Forest, OP: Open peatland

https://doi.org/10.5194/egusphere-2026-2272
Preprint. Discussion started: 29 April 2026

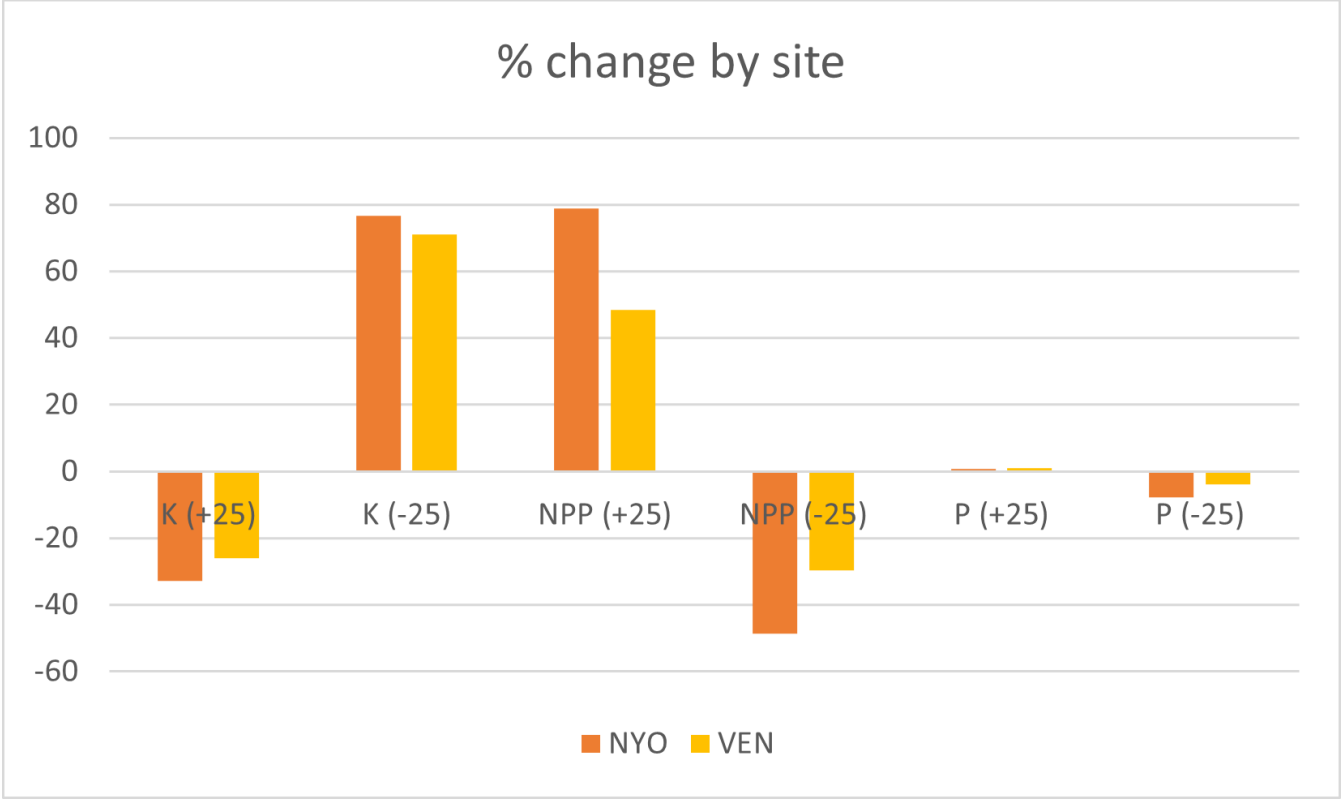

Figure B3. Sensitivity analysis for each site Nueva York (NYO-03) and Veinte de Enero (VEN-02) when parameters such as initial decomposition rate (k), Net Primary Productivity(NPP), and precipitation (P) are varied by ±25%

https://doi.org/10.5194/egusphere-2026-2272
Preprint. Discussion started: 29 April 2026

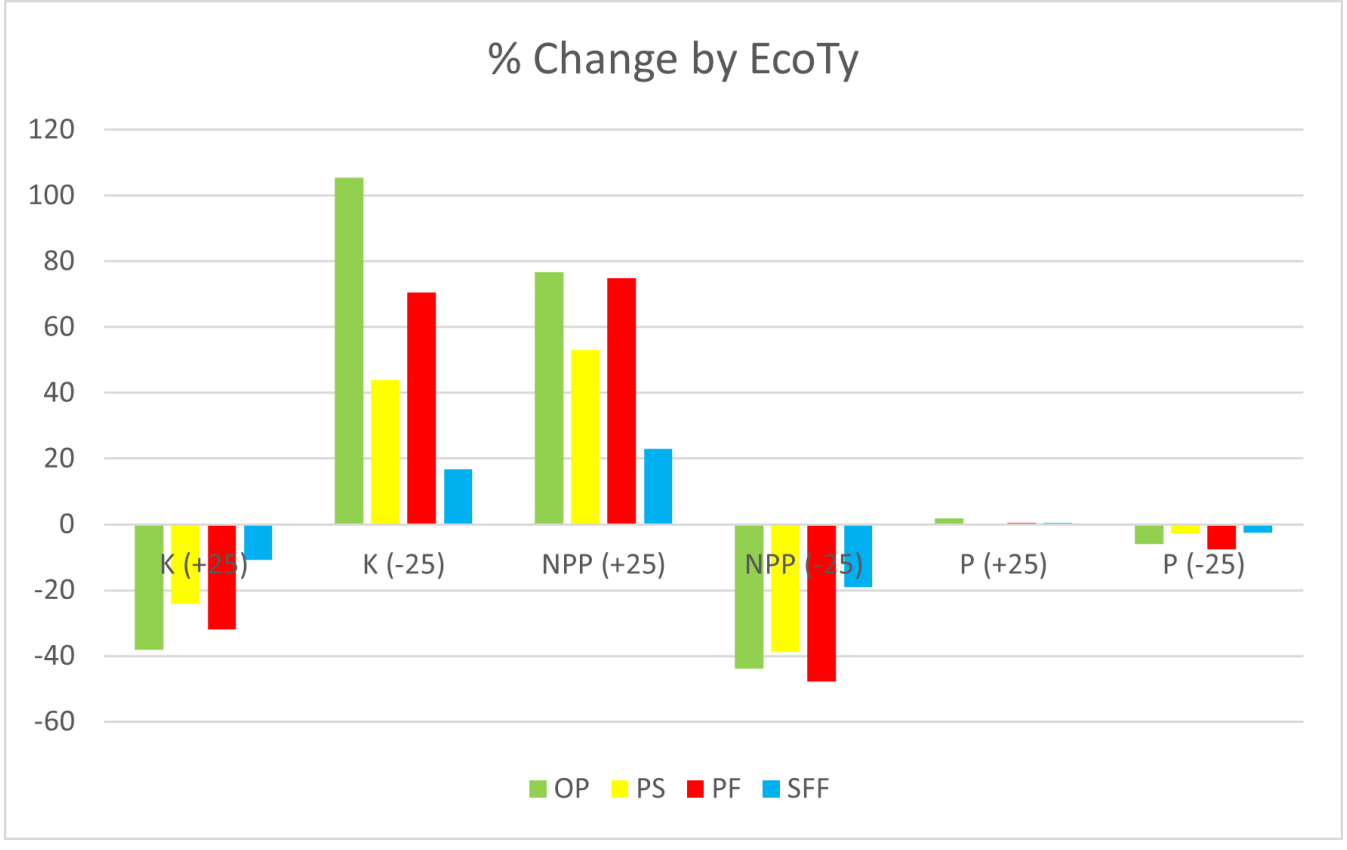

Figure B4. Sensitivity analysis by ecosystem type (EcoTy) when parameters such as initial decomposition rate (k), Net Primary Productivity(NPP), and precipitation (P) are varied by ±25%. PF: Pole Forest, PS: Palm Swamp, SFF: Seasonal Flooded Forest, OP: Open peatland

https://doi.org/10.5194/egusphere-2026-2272
Preprint. Discussion started: 29 April 2026

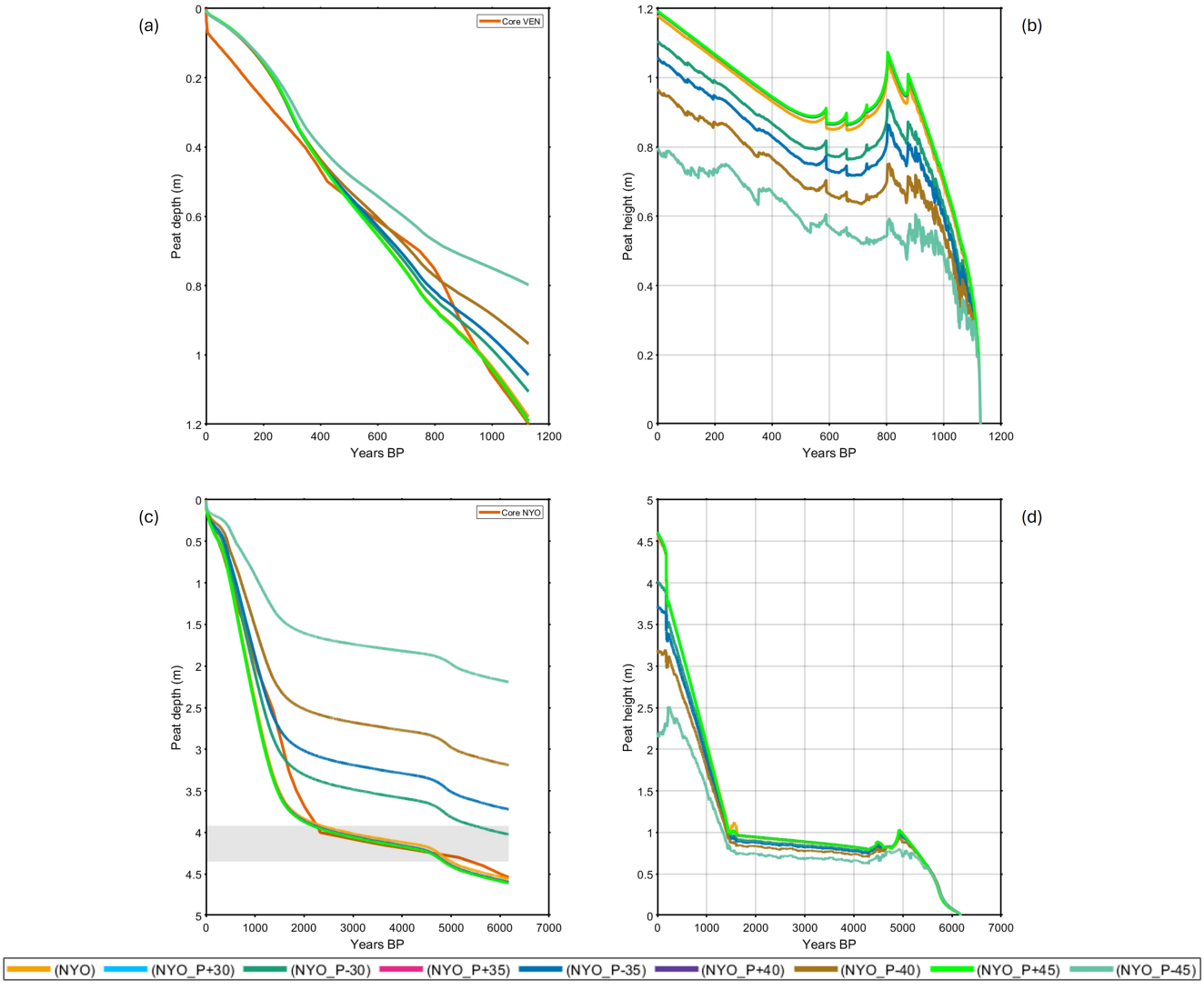

Figure B5. Precipitation sensitivity analysis for the sites Nueva York-03 (NYO-03) and Veinte de Enero-02 (VEN-02). Precipitation was varied from 30% to 45% in increments of 5% and the corresponding responses in peat depth and peat height were analysed. Plots (a) and (b) corresponds to the variation response in the peat depth and peat height curves respectively at NYO-03. Plots (c) and (d) corresponds to the variation response in the peat depth and peat height curves respectively at VEN-02

https://doi.org/10.5194/egusphere-2026-2272
Preprint. Discussion started: 29 April 2026

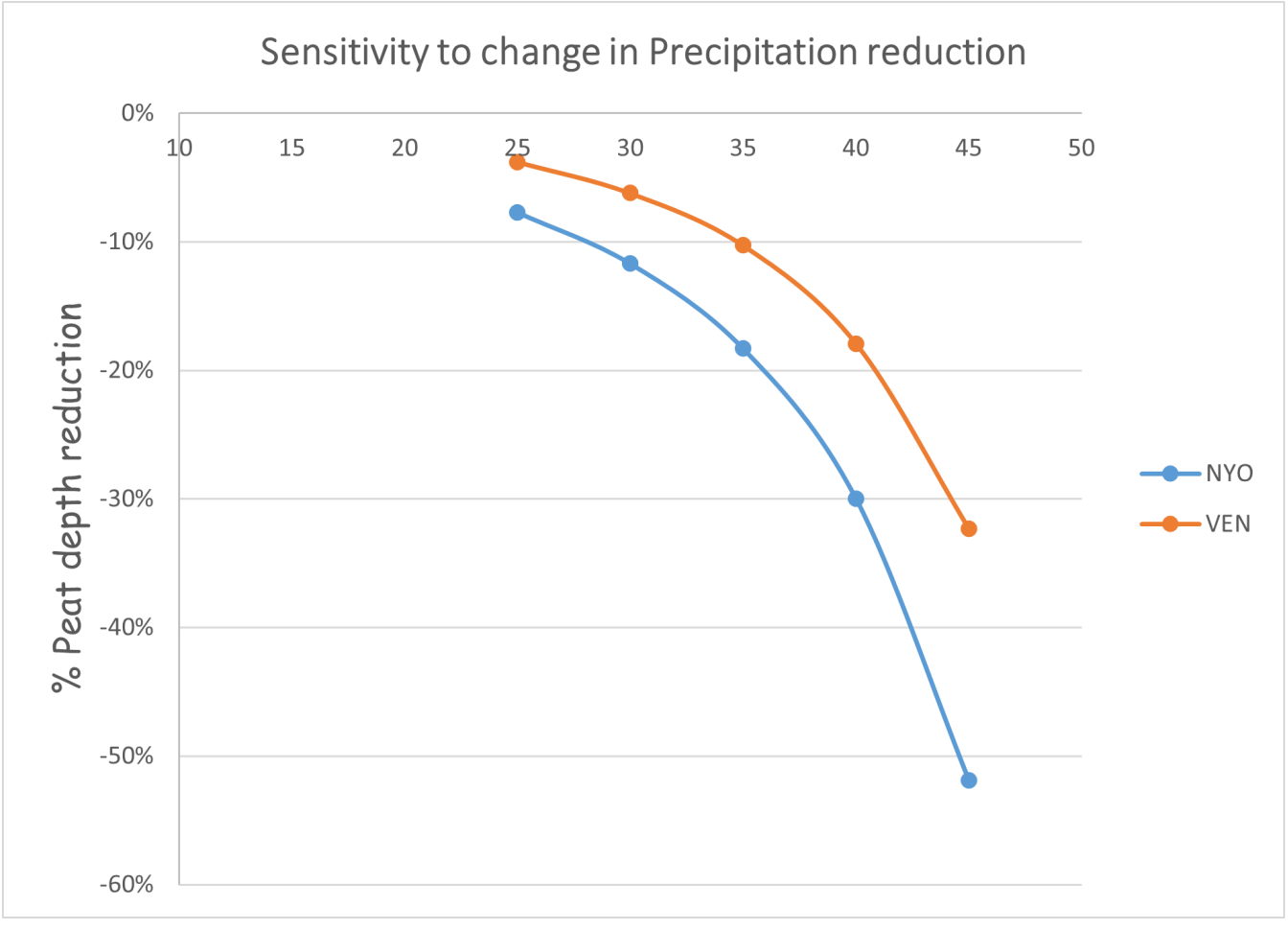

Figure B6. response trend of peat depth at the sites Nueva York-03 (NYO-03) and Veinte de Enero-02 (VEN-02) under precipitation reduction from 30% to 45% in increments of 5%

https://doi.org/10.5194/egusphere-2026-2272
Preprint. Discussion started: 29 April 2026

Author contributions. Yarin T. Puerta: Data curation; formal analysis; investigation; methodology; software; visualization; writing original draft; writing-review and editing. Ian T. Lawson: Conceptualization; funding acquisition; methodology; supervision; review and editing. Steve Frolking: Conceptualization; methodology; software; supervision; writing-original draft; writing-review and editing. Greta C. Dargie: Data curation; formal analysis; writing-review and editing. Jhon delÁguila Pasquel: Data curation. Christine Åkesson: Data curation; review and editing. Katy Roucoux: Conceptualization; writing-review and editing. Eurídice N. Honorio Coronado: writing-review and editing. Gerardo Flores Llampazo: Data curation. Timothy R. Baker: Data curation; writing-review. Mario A. Ruiz: Investigation; formal analysis; software; visualization, writing-review. Adam Hastie: Conceptualization; funding acquisition; project administration; formal analysis; methodology, software, writing-original draft; writing-review and editing.

Competing interests. The authors declare no competing interests are present.

Acknowledgements. We gratefully acknowledge the following funding: Charles University (PRIMUS/23/SCI/013), Grant Agency of Charles University (GAUK), project no. [448325], the Charles University Research Centre programme (UNCE/24/SCI/006), the Charles University/University of St Andrews Joint Seed Funding Scheme, the Johannes Amos Comenius Programme (P JAC), project No. CZ.02.01.01/00/22-_008/0004605, 'Natural and anthropogenic georisks', the Natural Environment Research Council (NERC: NE/R000751/1). We would like to thank Tyler Roman from USDA-Forest Service- International Programs for the guidance with PE-QFR Flux tower information. We would like to thank the Servicio Nacional de Meteorología e Hidrología del Perú (SENAMHI) for provided hydrological and meteorological data from ground stations in the region of interest. Finally, we also would like to thank Audra Swan PhD student at Charles University for the chats and discussions during our coffee and group meetings.

https://doi.org/10.5194/egusphere-2026-2272
Preprint. Discussion started: 29 April 2026

References

Andriesse, J.: Nature and management of tropical peat soils, FAO Soils Bulletin 59, FA, Rome (1988), p. 165.

Aragão, L. E. O. C., Malhi, Y., Roman-Cuesta, R. M., Saatchi, S., Anderson, L. O., and Shimabukuro, Y. E.: Spatial patterns and fire response of recent Amazonian droughts, 34, https://doi.org/10.1029/2006gl028946, 2007.

Basuki, I., Kauffman, J. B., Peterson, J. T., Anshari, G. Z., and Murdiyarso, D.: Land Cover and Land Use Change Decreases Net Ecosystem Production in Tropical Peatlands of West Kalimantan, Indonesia, 12, 1587, https://doi.org/10.3390/f12111587, 2021.

Beisner, B. E.: Alternative Stable States, 3, 33.

Bottino, M. J., Nobre, P., Giarolla, E., da Silva Junior, M. B., Capistrano, V. B., Malagutti, M., Tamaoki, J. N., de Oliveira, B. F. A., and Nobre, C. A.: Amazon savannization and climate change are projected to increase dry season length and temperature extremes over Brazil, 14, https://doi.org/10.1038/s41598-024-55176-5, 2024.

Bourgeau-Chavez, L. L., Grelik, S. L., Battaglia, M. J., Leisman, D. J., Chimner, R. A., Hribljan, J. A., Lilleskov, E. A., Draper, F. C., Zutta, B. R., Hergoualc'h, K., Bhomia, R. K., and Lähteenoja, O.: Advances in Amazonian Peatland Discrimination With Multi-Temporal PALSAR Refines Estimates of Peatland Distribution, C Stocks and Deforestation, 9, https://doi.org/10.3389/feart.2021.676748, 2021.

Bruno, R. D., da Rocha, H. R., de Freitas, H. C., Goulden, M. L., and Miller, S. D.: Soil moisture dynamics in an eastern Amazonian tropical forest, 20, 2477–2489, https://doi.org/10.1002/hyp.6211, 2006.

Capps, K. A., Graça, M. A. S., Encalada, A. C., and Flecker, A. S.: Leaf-litter decomposition across three flooding regimes in a seasonally flooded Amazonian watershed, 27, 205–210, https://doi.org/10.1017/s0266467410000635, 2011.

Chen, D., Xia, S., Li, S., Ding, X., Zhang, S., Chen, H., and Wu, J.: Moderate size diversity of tree roots has largest effect on the carbon loss in tropical soils, 38, 363–373, https://doi.org/10.1111/1365-2435.14468, 2023.

Clymo, R.: Models of Peat Growth, 43, 127–136.

Crezee, B., Dargie, G. C., Ewango, C. E. N., Mitchard, E. T. A., Emba B., O., Kanyama T., J., Bola, P., Ndjango, J.-B. N., Girkin, N. T., Bocko, Y. E., Ifo, S. A., Hubau, W., Seidensticker, D., Batumike, R., Imani, G., Cuní-Sanchez, A., Kiahtipes, C. A., Lebamba, J., Wotzka, H.-P., Bean, H., Baker, T. R., Baird, A. J., Boom, A., Morris, P. J., Page, S. E., Lawson, I. T., and Lewis, S. L.: Mapping peat thickness and carbon stocks of the central Congo Basin using field data, 15, 639–644, https://doi.org/10.1038/s41561-022-00966-7, 2022.

Cui, S., Liu, P., Guo, H., Nielsen, C. K., Pullens, J. W. M., Chen, Q., Pugliese, L., and Wu, S.: Wetland hydrological dynamics and methane emissions, 5, https://doi.org/10.1038/s43247-024-01635-w, 2024.

Cusack, D. F., Dietterich, L. H., and Sulman, B. N.: Soil Respiration Responses to Throughfall Exclusion Are Decoupled From Changes in Soil Moisture for Four Tropical Forests, Suggesting Processes for Ecosystem Models, 37, https://doi.org/10.1029/2022gb007473, 2023.

Dargie, G. C., del Aguila-Pasquel, J., Córdova Oroche, C. J., Irarica Pacaya, J., Reyna Huaymacari, J., Baker, T. R., Hastie, A., Honorio Coronado, E. N., Lewis, S. L., Roucoux, K. H., Mitchard, E. T., Williams, M., Draper, F. C. H., and Lawson, I. T.: Net primary productivity and litter decomposition rates in two distinct Amazonian peatlands, 30, https://doi.org/10.1111/gcb.17436, 2024.

de Meteorología e Hidrología del Perú (SENAMHI), S. N.: Datos Meteorológicos, https://www.senamhi.gob.pe/site/descarga-datos.

Dean, J. F., Coxon, G., Zheng, Y., Bishop, J., Garnett, M. H., Bastviken, D., Galy, V., Spencer, R. G. M., Tank, S. E., Tipper, E. T., Vonk, J. E., Wallin, M. B., Zhang, L., Evans, C. D., and Hilton, R. G.: Old carbon routed from land to the atmosphere by global river systems, 642, 105–111, https://doi.org/10.1038/s41586-025-09023-w, 2025.

del Aguila-Pasquel, J., Doughty, C. E., Metcalfe, D. B., Silva-Espejo, J. E., Girardin, C. A., Chung Gutierrez, J. A., Navarro-Aguilar, G. E., Quesada, C. A., Hidalgo, C. G., Reyna Huaymacari, J. M., Halladay, K., del Castillo Torres, D., Phillips, O., and Malhi, Y.: The seasonal

https://doi.org/10.5194/egusphere-2026-2272
Preprint. Discussion started: 29 April 2026

cycle of productivity, metabolism and carbon dynamics in a wet aseasonal forest in north-west Amazonia (Iquitos, Peru), 7, 71–83, https://doi.org/10.1080/17550874.2013.798365, 2013.

Dezzeo, N., Grandez-Rios, J., Martius, C., and Hergoualc'h, K.: Degradation-driven changes in fine root carbon stocks, productivity, mortality, and decomposition rates in a palm swamp peat forest of the Peruvian Amazon, 16, https://doi.org/10.1186/s13021-021-00197-0, 2021.

dos Reis, M., Graça, P. M. L. d. A., Yanai, A. M., Ramos, C. J. P., and Fearnside, P. M.: Forest fires and deforestation in the central Amazon: Effects of landscape and climate on spatial and temporal dynamics, 288, 112 310, https://doi.org/10.1016/j.jenvman.2021.112310, 2021.

Draper, F. C., Honorio Coronado, E. N., Roucoux, K. H., Lawson, I. T., A. Pitman, N. C., A. Fine, P. V., Phillips, O. L., Torres Montenegro, L. A., Valderrama Sandoval, E., Mesones, I., García-Villacorta, R., Arévalo, F. R. R., and Baker, T. R.: Peatland forests are the least diverse tree communities documented in Amazonia, but contribute to high regional beta-diversity, 41, 1256–1269, https://doi.org/10.1111/ecog.03126, 2018.

Evans, C. D., Page, S. E., Jones, T., Moore, S., Gauci, V., Laiho, R., Hruška, J., Allott, T. E. H., Billett, M. F., Tipping, E., Freeman, C., and Garnett, M. H.: Contrasting vulnerability of drained tropical and high-latitude peatlands to fluvial loss of stored carbon, 28, 1215–1234, https://doi.org/10.1002/2013gb004782, 2014.

Flores, B. M., Montoya, E., Sakschewski, B., Nascimento, N., Staal, A., Betts, R. A., Levis, C., Lapola, D. M., Esquível-Muelbert, A., Jakovac, C., Nobre, C. A., Oliveira, R. S., Borma, L. S., Nian, D., Boers, N., Hecht, S. B., ter Steege, H., Arieira, J., Lucas, I. L., Berenguer, E., Marengo, J. A., Gatti, L. V., Mattos, C. R. C., and Hirota, M.: Critical transitions in the Amazon forest system, 626, 555–564, https://doi.org/10.1038/s41586-023-06970-0, 2024.

Flores Llampazo, G., Honorio Coronado, E. N., del Aguila-Pasquel, J., Cordova Oroche, C. J., Díaz Narvaez, A., Reyna Huaymacari, J., Grandez Ríos, J., Lawson, I. T., Hastie, A., Baird, A. J., and Baker, T. R.: The presence of peat and variation in tree species composition are under different hydrological controls in Amazonian wetland forests, 36, https://doi.org/10.1002/hyp.14690, 2022.

Fonseca, L. D. M., Dalagnol, R., Malhi, Y., Rifai, S. W., Costa, G. B., Silva, T. S. F., Da Rocha, H. R., Tavares, I. B., and Borma, L. S.: Phenology and Seasonal Ecosystem Productivity in an Amazonian Floodplain Forest, 11, 1530, https://doi.org/10.3390/rs11131530, 2019.

Frolking, S., Roulet, N. T., Moore, T. R., Richard, P. J. H., Lavoie, M., and Muller, S. D.: Modeling Northern Peatland Decomposition and Peat Accumulation, 4, 479–498, https://doi.org/10.1007/s10021-001-0105-1, 2001.

Frolking, S., Roulet, N. T., Tuittila, E., Bubier, J. L., Quillet, A., Talbot, J., and Richard, P. J. H.: A new model of Holocene peatland net primary production, decomposition, water balance, and peat accumulation, 1, 1–21, https://doi.org/10.5194/esd-1-1-2010, 2010.

Frolking, S., Milliman, T., Palace, M., Wisser, D., Lammers, R., and Fahnestock, M.: Tropical forest backscatter anomaly evident in SeaWinds scatterometer morning overpass data during 2005 drought in Amazonia, 115, 897–907, https://doi.org/10.1016/j.rse.2010.11.017, 2011.

Frolking, S., Talbot, J., and Subin, Z. M.: Exploring the relationship between peatland net carbon balance and apparent carbon accumulation rate at century to millennial time scales, 24, 1167–1173, https://doi.org/10.1177/0959683614538078, 2014.

Garcin, Y., Schefuß, E., Dargie, G. C., Hawthorne, D., Lawson, I. T., Sebag, D., Biddulph, G. E., Crezee, B., Bocko, Y. E., Ifo, S. A., Mampouya Wenina, Y. E., Mbemba, M., Ewango, C. E. N., Emba, O., Bola, P., Kanyama Tabu, J., Tyrrell, G., Young, D. M., Gassier, G., Girkin, N. T., Vane, C. H., Adatte, T., Baird, A. J., Boom, A., Gulliver, P., Morris, P. J., Page, S. E., Sjögersten, S., and Lewis, S. L.: Hydroclimatic vulnerability of peat carbon in the central Congo Basin, 612, 277–282, https://doi.org/10.1038/s41586-022-05389-3, 2022.

Griffis, T., Roman, D., Wood, J., Deventer, J., Fachin, L., Rengifo, J., Del Castillo, D., Lilleskov, E., Kolka, R., Chimner, R., del Aguila-Pasquel, J., Wayson, C., Hergoualc'h, K., Baker, J., Cadillo-Quiroz, H., and Ricciuto, D.: Hydrometeorologi-

https://doi.org/10.5194/egusphere-2026-2272
Preprint. Discussion started: 29 April 2026

cal sensitivities of net ecosystem carbon dioxide and methane exchange of an Amazonian palm swamp peatland, 295, 108 167, https://doi.org/10.1016/j.agrformet.2020.108167, 2020.

Hajdu, L. H., Meesters, A. G. C. A., Dolman, A. J., and Friend, A. D.: Deforestation Could Push Amazonia Close to a Tipping Point Under Future Climate Change, 52, https://doi.org/10.1029/2024gl108304, 2025.

Hastie, A., Honorio Coronado, E. N., Reyna, J., Mitchard, E. T. A., Åkesson, C. M., Baker, T. R., Cole, L. E. S., Oroche, C. J. C., Dargie, G., Dávila, N., De Grandi, E. C., Del Águila, J., Del Castillo Torres, D., De La Cruz Paiva, R., Draper, F. C., Flores, G., Grández, J., Hergoualc'h, K., Householder, J. E., Janovec, J. P., Lähteenoja, O., Reyna, D., Rodríguez-Veiga, P., Roucoux, K. H., Tobler, M., Wheeler, C. E., Williams, M., and Lawson, I. T.: Risks to carbon storage from land-use change revealed by peat thickness maps of Peru, 15, 369–374, https://doi.org/10.1038/s41561-022-00923-4, 2022.

Hastie, A., Householder, J. E., Honorio Coronado, E. N., Hidalgo Pizango, C. G., Herrera, R., Lähteenoja, O., de Jong, J., Winton, R. S., Aymard Corredor, G. A., Reyna, J., Montoya, E., Paukku, S., Mitchard, E. T. A., Åkesson, C. M., Baker, T. R., Cole, L. E. S., Córdova Oroche, C. J., Dávila, N., Águila, J. D., Draper, F. C., Fluet-Chouinard, E., Grández, J., Janovec, J. P., Reyna, D., W Tobler, M., Del Castillo Torres, D., Roucoux, K. H., Wheeler, C. E., Fernandez Piedade, M. T., Schöngart, J., Wittmann, F., van der Zon, M., and Lawson, I. T.: A new data-driven map predicts substantial undocumented peatland areas in Amazonia, 19, 094 019, https://doi.org/10.1088/1748-9326/ad677b, 2024.

Hergoualc'h, K., Gutiérrez-Vélez, V. H., Menton, M., and Verchot, L. V.: Characterizing degradation of palm swamp peatlands from space and on the ground: An exploratory study in the Peruvian Amazon, 393, 63–73, https://doi.org/10.1016/j.foreco.2017.03.016, 2017.

Hergoualc'h, K., Dezzeo, N., Verchot, L. V., Martius, C., van Lent, J., del Aguila-Pasquel, J., and López Gonzales, M.: Spatial and temporal variability of soil N2O and CH4 fluxes along a degradation gradient in a palm swamp peat forest in the Peruvian Amazon, 26, 7198–7216, https://doi.org/10.1111/gcb.15354, 2020.

Hergoualc'h, K., van Lent, J., Dezzeo, N., Verchot, L. V., van Groenigen, J. W., López Gonzales, M., and Grandez-Rios, J.: Major carbon losses from degradation of Mauritia flexuosa peat swamp forests in western Amazonia, 167, 327–345, https://doi.org/10.1007/s10533-023-01057-4, 2023.

Hidalgo Pizango, C. G., Honorio Coronado, E. N., del Águila Pasquel, J., Flores Llampazo, G., de Jong, J., Córdova Oroche, C. J., Reyna Huaymacari, J. M., Carver, S. J., del Castillo Torres, D., Draper, F. C., Phillips, O. L., Roucoux, K. H., de Bruin, S., Peña-Claros, M., van der Zon, M., Mitchell, G., Lovett, J., García Mendoza, G., Gatica Saboya, L., Irarica Pacaya, J., Brañas, M. M., Ramírez Paredes, E., and Baker, T. R.: Sustainable palm fruit harvesting as a pathway to conserve Amazon peatland forests, 5, 479–487, https://doi.org/10.1038/s41893-022-00858-z, 2022.

Hirano, T., Segah, H., Kusin, K., Limin, S., Takahashi, H., and Osaki, M.: Effects of disturbances on the carbon balance of tropical peat swamp forests, 18, 3410–3422, https://doi.org/10.1111/j.1365-2486.2012.02793.x, 2012.

Hodnett, M., da Silva, L., da Rocha, H., and Cruz Senna, R.: Seasonal soil water storage changes beneath central Amazonian rainforest and pasture, 170, 233–254, https://doi.org/10.1016/0022-1694(94)02672-x, 1995.

Honorio Coronado, E. N., Hastie, A., Reyna, J., Flores, G., Grández, J., Lähteenoja, O., Draper, F. C., Åkesson, C. M., Baker, T. R., Bhomia, R. K., Cole, L. E. S., Dávila, N., Del Águila, J., Del Águila, M., Del Castillo Torres, D., Lawson, I. T., Martín Brañas, M., Mitchard, E. T. A., Monteagudo, A., Phillips, O. L., Ramírez, E., Ríos, M., Ríos, S., Rodriguez, L., Roucoux, K. H., Tagle Casapia, X., Vasquez, R., Wheeler, C. E., and Montoya, M.: Intensive field sampling increases the known extent of carbon-rich Amazonian peatland pole forests, 16, 074 048, https://doi.org/10.1088/1748-9326/ac0e65, 2021.

https://doi.org/10.5194/egusphere-2026-2272
Preprint. Discussion started: 29 April 2026

Hutyra, L. R., Munger, J. W., Nobre, C. A., Saleska, S. R., Vieira, S. A., and Wofsy, S. C.: Climatic variability and vegetation vulnerability in Amazônia, 32, https://doi.org/10.1029/2005gl024981, 2005.

Kalliola, R., Salo, J., Puhakka, M., Rajasilta, M., Häme, T., Neller, R. J., Räsänen, M. E., and Danjoy Arias, W. A.: Upper amazon channel migration: Implications for vegetation perturbance and succession using bitemporal landsat MSS images, 79, 75–79, https://doi.org/10.1007/bf01131806, 1992.

Kelly, T. J.: The long-term development of peatlands in Peruvian Amazonia, https://etheses.whiterose.ac.uk/id/eprint/9392/, accessed: 2025-02-12.

Kelly, T. J., Lawson, I. T., Roucoux, K. H., Baker, T. R., Jones, T. D., and Sanderson, N. K.: The vegetation history of an Amazonian domed peatland, 468, 129–141, https://doi.org/10.1016/j.palaeo.2016.11.039, 2017.

Kelly, T. J., Lawson, I. T., Roucoux, K. H., Baker, T. R., and Honorio Coronado, E. N.: Patterns and drivers of development in a west Amazonian peatland during the late Holocene, 230, 106 168, https://doi.org/10.1016/j.quascirev.2020.106168, 2020.

Kurnianto, S., Warren, M., Talbot, J., Kauffman, B., Murdiyarso, D., and Frolking, S.: Carbon accumulation of tropical peatlands over millennia: a modeling approach, 21, 431–444, https://doi.org/10.1111/gcb.12672, 2014.

Lavado Casimiro, W. S., Labat, D., Ronchail, J., Espinoza, J. C., and Guyot, J. L.: Trends in rainfall and temperature in the Peruvian Amazon–Andes basin over the last 40 years (1965–2007), 27, 2944–2957, https://doi.org/10.1002/hyp.9418, 2012.

Lawson, I., Åkesson, C., Dargie, G., del Aguila Pasquel, J., Draper, F., Hastie, A., Kelly, T., Sassoon, D., Abraham, V., Baker, T., Fabel, D., Gulliver, P., Honorio Coronado, E., and Roucoux, K.: Holocene patterns of peat accumulation in Peruvian Amazonia, 686, 113 579, https://doi.org/10.1016/j.palaeo.2026.113579, 2026.

Lawson, I. T., Honorio Coronado, E. N., Andueza, L., Cole, L., Dargie, G. C., Davies, A. L., Laurie, N., Okafor-Yarwood, I., Roucoux, K. H., and Simpson, M.: The vulnerability of tropical peatlands to oil and gas exploration and extraction, 1, 84–114, https://doi.org/10.1177/27539687221124046, 2022.

Lähteenoja, O., Ruokolainen, K., Schulman, L., and Oinonen, M.: Amazonian peatlands: an ignored C sink and potential source, 15, 2311–2320, https://doi.org/10.1111/j.1365-2486.2009.01920.x, 2009.

Lähteenoja, O., Reátegui, Y. R., Räsänen, M., Torres, D. D. C., Oinonen, M., and Page, S.: The large <scp>A</scp>mazonian peatland carbon sink in the subsiding <scp>P</scp>astaza-<scp>M</scp>arañón foreland basin, <scp>P</scp>eru, 18, 164–178, https://doi.org/10.1111/j.1365-2486.2011.02504.x, 2011.

Malhi, Y., Aragão, L. E. O. C., Galbraith, D., Huntingford, C., Fisher, R., Zelazowski, P., Sitch, S., McSweeney, C., and Meir, P.: Exploring the likelihood and mechanism of a climate-change-induced dieback of the Amazon rainforest, 106, 20 610–20 615, https://doi.org/10.1073/pnas.0804619106, 2009.

Martins, N. P., Valverde-Barrantes, O., Fuchslueger, L., Lugli, L. F., Grandis, A., Hofhansl, F., Takeshi, B., Ushida, G., and Quesada, C. A.: Fine root presence and increased phosphorus availability stimulate wood decay in a central Amazonian rainforest, 2024, https://doi.org/10.1111/oik.09996, 2023.

Mezbahuddin, M., Grant, R. F., and Hirano, T.: Modelling effects of seasonal variation in water table depth on net ecosystem CO2 exchange of a tropical peatland, 11, 577–599, https://doi.org/10.5194/bg-11-577-2014, 2014.

Morison, J., Piedade, M., Müller, E., Long, S., Junk, W., and Jones, M.: Very high productivity of the C4 aquatic grass Echinochloa polystachya in the Amazon floodplain confirmed by net ecosystem CO2 flux measurements, 125, 400–411, https://doi.org/10.1007/s004420000464, 2000.

https://doi.org/10.5194/egusphere-2026-2272
Preprint. Discussion started: 29 April 2026

Moyano, F. E., Manzoni, S., and Chenu, C.: Responses of soil heterotrophic respiration to moisture availability: An exploration of processes and models, 59, 72–85, https://doi.org/10.1016/j.soilbio.2013.01.002, 2013.

Page, S. and Rieley, J.: Tropical Peat Swamp Forests of Southeast Asia, pp. 1753–1761, Springer Netherlands, ISBN 9789400740013, https://doi.org/10.1007/978-94-007-4001-3_5, 2018.

Page, S. E., Rieley, J. O., Shotyk, Ø. W., and Weiss, D.: Interdependence of peat and vegetation in a tropical peat swamp forest, 354, 1885–1897, https://doi.org/10.1098/rstb.1999.0529, 1999.

Page, S. E., Rieley, J. O., and Banks, C. J.: Global and regional importance of the tropical peatland carbon pool, 17, 798–818, https://doi.org/10.1111/j.1365-2486.2010.02279.x, 2011.

Perryman, C. R., Baysinger, M. R., Cobb, A. R., Gandois, L., Chanton, J. P., Evans, T., Chua, A., Eri, J., Bohari bin Haji Idi, H., Incham, J. M., Pu, J. P., Teo, A., Zulkiflee, R. A., Harvey, C. F., and Hoyt, A. M.: Insights Into the Persistence and Vulnerability of Tropical Peat Carbon Stocks From a Long-Term Field Decomposition Experiment, 40, https://doi.org/10.1029/2025gb008821, 2026.

Quintana-Cobo, I., Moreira-Turcq, P., Cordeiro, R. C., Aniceto, K., Crave, A., Fraizy, P., Moreira, L. S., Duarte Contrera, J. M. d. A., and Turcq, B.: Dynamics of floodplain lakes in the Upper Amazon Basin during the late Holocene, 350, 55–64, https://doi.org/10.1016/j.crte.2017.10.004, 2018.

Roucoux, K., Lawson, I., Jones, T., Baker, T., Coronado, E. H., Gosling, W., and Lähteenoja, O.: Vegetation development in an Amazonian peatland, 374, 242–255, https://doi.org/10.1016/j.palaeo.2013.01.023, 2013.

Ríos-Villamizar, E. A., Adeney, J. M., Piedade, M. T. F., and Junk, W. J.: New insights on the classification of major Amazonian river water types, 6, https://doi.org/10.1007/s40899-020-00440-5, 2020.

Snyder, J. M. and Rejmánková, E.: Macrophyte root and rhizome decay: the impact of nutrient enrichment and the use of live versus dead tissue in decomposition studies, 124, 45–59, https://doi.org/10.1007/s10533-015-0080-9, 2015.

Sousa, T. R., Schietti, J., Ribeiro, I. O., Emílio, T., Fernández, R. H., ter Steege, H., Castilho, C. V., Esquivel-Muelbert, A., Baker, T., Pontes-Lopes, A., Silva, C. V. J., Silveira, J. M., Derroire, G., Castro, W., Mendoza, A. M., Ruschel, A., Prieto, A., Lima, A. J. N., Rudas, A., Araujo-Murakami, A., Gutierrez, A. P., Andrade, A., Roopsind, A., Manzatto, A. G., Di Fiore, A., Torres-Lezama, A., Dourdain, A., Marimon, B., Marimon, B. H., Burban, B., van Ulft, B., Herault, B., Quesada, C., Mendoza, C., Stahl, C., Bonal, D., Galbraith, D., Neill, D., de Oliveira, E. A., Hase, E., Jimenez-Rojas, E., Vilanova, E., Arets, E., Berenguer, E., Alvarez-Davila, E., Honorio Coronado, E. N., Almeida, E., Coelho, F., Valverde, F. C., Elias, F., Brown, F., Bongers, F., Arevalo, F. R., Lopez-Gonzalez, G., van der Heijden, G., Aymard C., G. A., Llampazo, G. F., Pardo, G., Ramírez-Angulo, H., do Amaral, I. L., Vieira, I. C. G., Huamantupa-Chuquimaco, I., Comiskey, J. A., Singh, J., Espejo, J. S., del Aguila-Pasquel, J., Zwerts, J. A., Talbot, J., Terborgh, J., Ferreira, J., Barroso, J. G., Barlow, J., Camargo, J. L., Stropp, J., Peacock, J., Serrano, J., Melgaço, K., Ferreira, L. V., Blanc, L., Poorter, L., Gamarra, L. V., Aragão, L., Arroyo, L., Silveira, M., Peñuela-Mora, M. C., Vargas, M. P. N., Toledo, M., Disney, M., Réjou-Méchain, M., Baisie, M., Kalamandeen, M., Camacho, N. P., Cardozo, N. D., Silva, N., Pitman, N., Higuchi, N., Banki, O., Loayza, P. A., Graça, P. M. L. A., Morandi, P. S., van der Meer, P. J., van der Hout, P., Naisso, P., Camargo, P. B., Salomão, R., Thomas, R., Boot, R., Umetsu, R. K., da Costa Silva, R., Burnham, R., Zagt, R., Martinez, R. V., Brienen, R., Ribeiro, S. C., Lewis, S. L., Vieira, S. A., de Almeida Reis, S. M., Fauset, S., Laurance, S., Feldpausch, T., Erwin, T., Killeen, T., Wortel, V., Moscoso, V. C., Vos, V., Huasco, W. H., Laurance, W., Malhi, Y., Magnusson, W. E., Phillips, O. L., and Costa, F. R. C.: Water table depth modulates productivity and biomass across Amazonian forests, 31, 1571–1588, https://doi.org/10.1111/geb.13531, 2022.

Souza, R. D. A. D., Moura, V., Paloschi, R. A., Aguiar, R. G., Webler, A. D., and Borma, L. D. S.: Assessing Drought Response in the Southwestern Amazon Forest by Remote Sensing and In Situ Measurements, 14, 1733, https://doi.org/10.3390/rs14071733, 2022.

https://doi.org/10.5194/egusphere-2026-2272
Preprint. Discussion started: 29 April 2026

Swindles, G. T., Morris, P. J., Whitney, B., Galloway, J. M., Gałka, M., Gallego-Sala, A., Macumber, A. L., Mullan, D., Smith, M. W., Amesbury, M. J., Roland, T. P., Sanei, H., Patterson, R. T., Sanderson, N., Parry, L., Charman, D. J., Lopez, O., Valderamma, E., Watson, E. J., Ivanovic, R. F., Valdes, P. J., Turner, T. E., and Lähteenoja, O.: Ecosystem state shifts during long-term development of an Amazonian peatland, 24, 738–757, https://doi.org/10.1111/gcb.13950, 2017.

Swinnen, W., Broothaerts, N., and Verstraeten, G.: Modelling long-term blanket peatland development in eastern Scotland, 16, 3977–3996, https://doi.org/10.5194/bg-16-3977-2019, 2019.

Tuittila, E.-S., Juutinen, S., Frolking, S., Väliranta, M., Laine, A. M., Miettinen, A., Seväkivi, M.-L., Quillet, A., and Merilä, P.: Wetland chronosequence as a model of peatland development: Vegetation succession, peat and carbon accumulation, 23, 25–35, https://doi.org/10.1177/0959683612450197, 2012.

Violita, V., Triadiati, T., Anas, I., and Miftahudin, M.: Fine Root Production and Decomposition in Lowland Rainforest and Oil Palm Plantations in Sumatra, Indonesia, 23, 7–12, https://doi.org/10.1016/j.hjb.2015.10.008, 2016.

Wang, B., Hapsari, K. A., Horna, V., Zimmermann, R., and Behling, H.: Late Holocene peatland palm swamp (aguajal) development, carbon deposition and environment changes in the Madre de Dios region, southeastern Peru, 594, 110 955, https://doi.org/10.1016/j.palaeo.2022.110955, 2022.

Wang, S., Zhuang, Q., Yu, Z., Bridgham, S., and Keller, J. K.: Quantifying peat carbon accumulation in Alaska using a process-based biogeochemistry model, 121, 2172–2185, https://doi.org/10.1002/2016jg003452, 2016.

Wang, S., Zhuang, Q., Lähteenoja, O., Draper, F. C., and Cadillo-Quiroz, H.: Potential shift from a carbon sink to a source in Amazonian peatlands under a changing climate, 115, 12 407–12 412, https://doi.org/10.1073/pnas.1801317115, 2018.

Warren, M., Frolking, S., Dai, Z., and Kurnianto, S.: Impacts of land use, restoration, and climate change on tropical peat carbon stocks in the twenty-first century: implications for climate mitigation, 22, 1041–1061, https://doi.org/10.1007/s11027-016-9712-1, 2016.

Wright, E. L., Black, C. R., Cheesman, A. W., Turner, B. L., and Sjögersten, S.: Impact of Simulated Changes in Water Table Depth on Ex Situ Decomposition of Leaf Litter from a Neotropical Peatland, 33, 217–226, https://doi.org/10.1007/s13157-012-0369-6, 2013.

Young, D. M., Baird, A. J., Gallego-Sala, A. V., and Loisel, J.: A cautionary tale about using the apparent carbon accumulation rate (aCAR) obtained from peat cores, 11, https://doi.org/10.1038/s41598-021-88766-8, 2021.

Young, D. M., Baird, A. J., Morris, P. J., Dargie, G. C., Mampouya Wenina, Y. E., Mbemba, M., Boom, A., Cook, P., Betts, R., Burke, E., Bocko, Y. E., Chadburn, S., Crabtree, D. E., Crezee, B., Ewango, C. E. N., Garcin, Y., Georgiou, S., Girkin, N. T., Gulliver, P., Hawthorne, D., Ifo, S. A., Lawson, I. T., Page, S. E., Jovani-Sancho, A. J., Schefuß, E., Sciumbata, M., Sjögersten, S., and Lewis, S. L.: Simulating carbon accumulation and loss in the central Congo peatlands, 29, 6812–6827, https://doi.org/10.1111/gcb.16966, 2023.